Modelling the spatial demography of Atlantic cod (*Gadus morhua*) on the European continental shelf

Jessica M. Andrews, William S.C. Gurney, Michael R. Heath, Alejandro Gallego, Carl M. O'Brien, Christopher Darby, and Graham Tyldesley

Abstract: Atlantic cod (*Gadus morhua*) stocks across the North Atlantic have been subject to intense fishing pressure during the 20th century, and some stocks have suffered well-documented collapses. On the European shelf, cod are widely but heterogeneously distributed and are caught as part of a multispecies trawl fishery. There is a growing body of evidence that this stock is composed of substocks with potentially distinct demographic properties. As a first step towards the development of management methodologies that reflect this spatial and biological complexity, we present a spatially and physiologically explicit model describing the demography and distribution of cod on the European shelf. The computational efficiency of our implementation enables numerical parameter optimization, thus facilitating formal statistical tests of structural hypotheses. We use these methods to fit model variants embodying a variety of hypotheses about the movements of settled fish to a data set including spatial distribution information derived from International Bottom Trawl Surveys. The best-fit model emerging from this study is then used to investigate the potential effects of long-term application of a series of regional fishing closure policies.

Résumé : Les stocks de morues franches (*Gadus morhua*) dans tout l'Atlantique Nord ont subi une pression de pêche intense durant le 20ᵉ siècle et certains d'entre eux ont connu des effondrements bien documentés. Sur la plate-forme européenne, les morues sont réparties de manière étendue mais hétérogène et sont capturées dans le cadre de pêches multispécifiques au chalut. Il y a de plus en plus d'indications que ce stock est composés de sous-stocks possédant des propriétés démographiques distinctes. Comme première étape de la mise en place de méthodologies de gestion qui reflètent cette complexité spatiale et biologique, nous présentons un modèle explicite des points de vue spatial et physiologique qui décrit la démographie et la répartition des morues sur la plate-forme européenne. L'efficacité informatique de notre méthodologie permet une optimisation numérique des paramètres, facilitant ainsi l'application de tests statistiques formels aux hypothèses structurales. Nous utilisons ces méthodes pour ajuster à une banque de données provenant des inventaires internationaux au chalut de fond plusieurs variantes du modèle relatives à une gamme d'hypothèses sur les déplacements des poissons après leur établissement. Le modèle qui produit le meilleur ajustement dans notre étude a ensuite servi à déterminer les effets potentiels d'une mise en application de diverses politiques de fermeture régionale de la pêche sur une longue période.

[Traduit par la Rédaction]

Introduction

Atlantic cod (*Gadus morhua*; hereafter referred to as cod) stocks across the entire geographic range in the North Atlantic were subjected to intense fishing pressure during the 20th century and many suffered well-documented collapses. Subsequent analyses have shown that in some outstanding cases (e.g., the northwestern cod stock off Newfoundland), the terminal collapse was probably due to a combination of overfishing and adverse climate (Rose 2004). In this case, even a total cessation of fishing does not seem to have promoted recovery, most likely because of depensatory effects resulting from of low stock numbers (Frank and Brickman 2000).

It is feared that a similar train of events to those seen off Newfoundland may be taking place in European waters. Fishing mortality rates that were considered sustainable during the 1960s and 1970s are no longer so today because of a decline in productivity linked to climate change. In the case of the North Sea, the climatic link is manifest as a negative correlation between recruitment and sea temperature

J.M. Andrews and G. Tyldesley. Department of Statistics and Modelling Science, University of Strathclyde, Glasgow G1 1XH, Scotland.
**W.S.C. Gurney.**[1] Fisheries Research Services (FRS) Marine Laboratory, Aberdeen AB11 9DB, Scotland; and Department of Statistics and Modelling Science, University of Strathclyde, Glasgow G1 1XH, Scotland.
R. Heath and A. Gallego. Fisheries Research Services (FRS) Marine Laboratory, Aberdeen AB11 9DB, Scotland.
C.M. O'Brien and C. Darby. Centre for Environment, Fisheries & Aquaculture Science (Cefas), Lowestoft Laboratory, Pakefield Road, Lowestoft, Suffolk NR33 OHT, England.

[1]Corresponding author (e-mail: bill@stams.strath.ac.uk).

Fig. 1. The European shelf area covered by this study, showing the 200 m contour that we take to define the edge of the continental shelf and assessment region boundaries (straight solid lines).
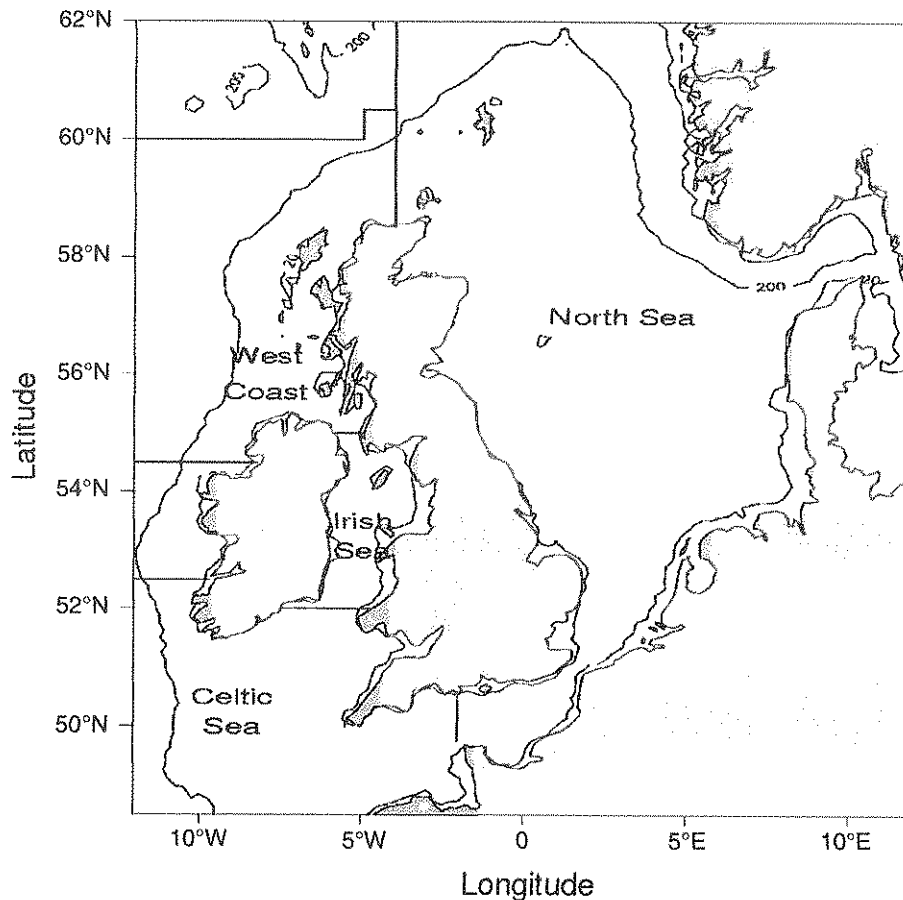
(O'Brien et al. 2000), which is in turn linked to the North Atlantic Oscillation Index (Planque and Frédou 1999; Beaugrand et al. 2003; Brander and Mohn 2004). The increasing unsustainability of harvesting rates was recognised in the late 1990s (Cook et al. 1997), and in 2001 a trial closure of certain spawning grounds was imposed, with a total cessation of fishing for cod being recommended in 2002 (ICES 2003).

Unlike the situation in Newfoundland, cod in European waters (Fig. 1) are caught largely as part of a multispecies trawl fishery rather than as a single-species targeted fishery. Hence, a total cessation of fishing for North Sea cod was technically difficult to implement without effectively imposing a ban on all mixed roundfish fisheries. Instead, the closure of selected fishing grounds in 2001 has been developed as part of a cod recovery plan, whereby trawling was prohibited in areas and at times when cod were thought to predominate in the demersal fish assemblage. However, it has long been suspected that cod is a population-rich species with complex spatial structure (Sinclair 1988), and since all of the population models of cod available at the time were based on whole-stock, spatially aggregated dynamics, prognoses of the likely impact of these spatially structured closure plans could, at best, be considered to be only very approximate.

Fishermen have known for centuries that cod migrate annually to particular locations to spawn (Kurlanski 1999), and tagging studies from across the North Atlantic indicate a high degree of spawning site fidelity among repeat-spawning fish. A high proportion of fish tagged on a spawning site at spawning time and recovered at spawning time in subsequent years are usually recovered within a short radius of their original tagging location, while recoveries at other times of year may have moved considerable distances (Robichaud and Rose 2001, 2004). At the same time, it is clear that there are regional differences in demography and phenotypic properties of fish, which seem to be related to the different spawning regions (West 1970; Yoneda and Wright 2004). The impression is that cod stocks may exhibit a metapopulation structure at a smaller scale than the stock assessment units, maintained by the extent of mixing through passive transport of eggs and larvae and by migrations of juveniles and adults.

Tagging studies cannot give insight on the extent to which apparently distinct spawning populations may be reproductively isolated (i.e., whether the return migration of adults to particular spawning sites represents natal fidelity). Early attempts at allozyme-based genetic studies indicated that in the North Sea, cod were a single, panmictic unit (Jamieson

and Thompson 1972; Child 1988). However, more recently, Hutchinson et al. (2001) investigated microsatellite DNA markers and found four genetically distinct groups centred on Bergen Bank, Moray Firth, Flamborough Head, and the Southern Bight, which broadly map onto the groupings emerging from tagging studies. Differentiation was weak but significant, and the degree of genetic isolation was weakly correlated with the geographical separation distance. Hence, the implication was that the cycle of spawning, larval drift, and juvenile and adult migration is self-contained over the geographical scale of each of these populations, with relatively little leakage. Long-term changes (1954–1998) in genetic structuring have also been examined by DNA analysis of archived otoliths from the Flamborough Head population (Hutchinson et al. 2003). These data indicated marked genetic changes and loss of allelic diversity during a period of major decline in abundance.

Thus, although the evidence is fragmentary, the combination of tagging and genetic and morphometric data suggests that cod in European waters are certainly not homogeneously mixed and that the essential spatial scale of breeding populations is smaller than the current stock assessment units, being defined by some function of larval drift and juvenile and adult migration patterns. Hence, recovery plans involving spatially structured fishery prohibitions may have unforeseen consequences depending on their placement, and any benefits may not be distributed equally over the current assessment regions. Models to predict such consequences will need to represent the physical oceanographic features and fish behavior patterns that maintain spatial organisation, as well as the spatial patterns of production (recruitment and growth) and mortality (natural and fishing), and how all of these may have changed over time in response to climate fluctuations. This represents a substantial departure from the current modelling approaches as applied to fish stocks. In this paper, we describe a model having the necessary spatial properties and present some simulated prognoses of the consequences of different fishery closure strategies.

The model

The biology of cod

The cod life cycle (Fig. 2) begins in the spawning season (February–April; Brander 1994) with the release of eggs, which float at or near the surface, drifting with the prevailing current. After a temperature-dependent incubation period (Page and Frank 1989), surviving eggs hatch into larvae, which feed and grow into juvenile fish (Brander 1994; Brander and Mohn 2004).

Larvae and early juveniles are active swimmers who reside deeper in the water column than eggs (Heath et al. 2003). However, given their small size (<3.5 cm), the midwater currents to which they are exposed must still be the principal determinant of long-term movement.

Pelagic juveniles whose length exceeds 3.5 cm move down the water column to seek a region where they can begin demersal life, where lower current speeds and increasing body size combine to imply that long-term relocation is likely to be largely facultative (see Brander 1994; Robichaud and Rose 2004). Settled juveniles have lower natural mortal-

Fig. 2. The Atlantic cod (*Gadus morhua*) life cycle.
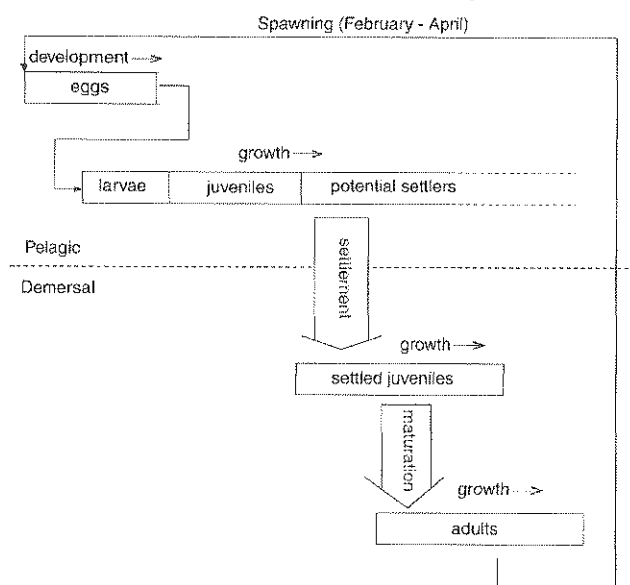
ity than pelagic juveniles and grow rapidly, becoming vulnerable to commercial fishing at a size that depends on the local regulatory framework, but is generally ~20 cm. Surviving individuals eventually mature into reproductively active adults, who continue to grow and spawn yearly until death, with large females being considerably more fecund than small ones (Marteinsdottir and Begg 2002).

A discrete space–time framework

The model described in this paper uses an extension of the discrete space–time methodology proposed by Gurney et al. (2001) and used by Speirs et al. (2005) to model the basin-scale demography of *Calanus finmarchicus*. In the following sections, we give a qualitative discussion of the application of this methodology to *G. morhua*. Full mathematical detail is given in Appendix A.

The first key to this methodology is to divide the individual's life history into segments within which each individual interacts with its physical and biotic environment according to the same rules. For example, as a reasonable modelling approximation, we can regard all eggs as being located at a fixed depth, so that all eggs in a given cell are subject to a uniform hydrodynamic and temperature environment. Our life cycle description (Fig. 2) contains four such segments. Eggs are differentiated from all other individuals in having development rates determined solely by temperature. Pelagic juveniles have the same development rules as settled individuals but are subject to different hydrodynamic environments. Settled juveniles and adults are distinguished by the fact that adults reproduce.

The second key requirement is that the development of an individual through any given segment is described by a single index. For example, if we assume that differences in condition between adult individuals can be neglected, then individual demographic properties can reasonably be thought of as being determined by a single measure of size. Within a given segment, individuals are assigned to discrete develop-

ment classes chosen to have the property that survivors of the group of individuals in a given class at a given biological update are obligate members of the next class at the succeeding biological update.

Our model covers the region from 40°30′N to 62°N and from 12°W to 12°E (Fig. 1) using cells that cover four International Council for the Exploration of the Sea (ICES) squares (each cell = 1°N × 2°W). For any given segment, physical transport is described by a transfer matrix, which defines the probability that an individual in a given development class in that cell at one transport update is relocated to another spatial cell by the next transport update.

Gurney et al. (2001) showed that a scheme that treats each cell as autonomous between transport updates will produce results extremely close to the solution of the equivalent partial differential equation description provided only that development class width is small enough for biological updates to occur much more frequently than transport updates. They also demonstrated that the payoff from using their methodology is that the computations are three to five orders of magnitude faster than the partial differential equation solution, thus permitting spatial demographic models to be used within numerical optimization algorithms.

Development

Page and Frank (1989) have shown that the time between deposition and hatching of cod eggs is dependent on water temperature, so we classify individuals by the currently achieved proportion of development between release and hatch — an index which obviously runs from 0 to 1 — and seek an appropriately temperature-dependent development rate. We write this development rate as

$$(1) \qquad g_x^E(t) = D_E(T_x(t) + T_E)^{P_E}$$

and we exploit the work of Daan (1978) and Fox et al. (2000), who have pointed out the similarity between the eggs of cod and haddock, to obtain the parameter values given in Appendix A.

For all life-history segments except eggs, we classify individuals by their length (L) and assume that growth follows the pattern described by von Bertalanffy (1957), that is

$$(2) \qquad \frac{dL}{dt} = g_x(L_\infty - L)$$

where g_x is the local growth rate in cell x. To obtain a position-independent development index (q), we assume that the asymptotic length (L_∞) and the length at hatch (L_H) are uniform across the domain and define

$$(3) \qquad q \equiv \ln\left(\frac{L_\infty - L_H}{L_\infty - L}\right)$$

This implies that q runs from 0 when an individual is recruited after hatch, to ∞ for an individual who has reached L_∞, and that q changes at a cell-dependent rate

$$(4) \qquad \frac{dq}{dt} = g_x$$

To determine g_x, we fitted von Bertalanffy growth curves with common L_∞ and L_H and cell-dependent growth rate to a

data set of sex–maturity age–length keys compiled from information provided by ICES (the International Bottom Trawl Surveys, IBTS), Fisheries Research Services (Marine Laboratory, Aberdeen, Scotland), the Centre for Ecology, Fisheries and Aquaculture Science (Lowestoft, England), and the Department of Agriculture and Regional Development (Dundonald House, Belfast, Northern Ireland).

We illustrate the quality of fit thus obtained (Fig. 3) and show a grey-scale map of the best-fit growth rates for all stat squares with significant data content (Fig. 4a). To infill the cells for which insufficient data is available to permit satisfactory fitting, we use a generalized additive model ($R^2 = 0.72$) of growth rate against latitude, longitude, and mean annual temperature obtained from the statistical analysis reported by Heath et al. (2003). The final result is shown in Fig. 4b. To check the validity of our assumption that L_∞ is spatially uniform, we repeat the above fitting exercise with cell-dependent L_∞ and find no large improvement in fit quality.

Progression through the life history

Eggs are recruited at 0 development index and hatch when $q^E = 1$, so at constant temperature (T) the time (τ_H) between release and hatch is

$$(5) \qquad T_E = \frac{1}{D_E(T_x(t) + T_E)^{P_E}}$$

At hatch, individuals are recruited to the pelagic juvenile segment at development index 0 (length = L_H) and develop according to eq. (2).

When a pelagic juvenile reaches a length $L_S = 3.5$ cm, it becomes eligible for transfer to the settled juvenile segment. This transfer occurs if it currently occupies a cell with finite area in the depth range 25–200 m.

Prior to the start of each spawning season, a proportion $m(L(q))$ of each settled juvenile development class is transferred to the equivalent settled adult class. To determine the proportion mature at length, $m(L)$ (Fig. 5a), we use a Weibull fit to the ICES estimates of proportion mature at age for the whole North Sea, which we transform using a whole North Sea age–length key (see Appendix A). We show (Fig. 5b) the implied equivalent maturity at age curves for individuals growing at the fastest and slowest rates from Fig. 4. At the slowest rate, which is comparable with the values over a large part of the central-eastern North Sea, the time for 90% of the cohort to mature is around 7 years, which is consistent with the observation (ICES 2001a) that over the whole North Sea the average time for stock maturity is 6 years. At the fastest rate, which occurs in the south Irish Sea, the time to 90% maturity is a little less than 4 years, which is consistent with observations (ICES 2001b) that Irish Sea stock matures in about 3 years, while Celtic Sea stock matures in around 5 years.
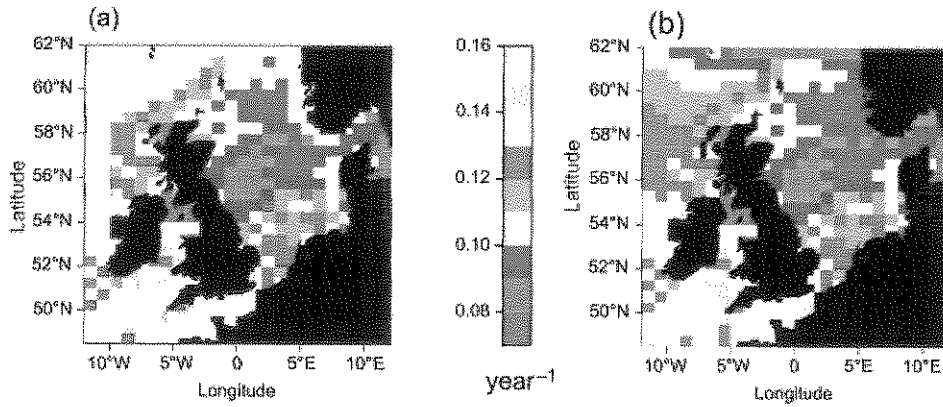
Mortality

Natural mortality

To calculate the daily mortality rate for eggs (0.232·day⁻¹), we used the relationship between egg size and mortality given by Rijnsdorp and Jaworski (1990) with an assumed egg diameter of 1.4 mm. For settled individuals in both juve-

Fig. 3. Fitted von Bertalanffy curves for representative International Council for the Exploration of the Sea (ICES) rectangles. Best-fit global values of length at hatch (L_H) and at $t = \infty$ (L_∞) are 0.14 and 197 cm, respectively. (*a*) ICES square 43E8: growth rate = 0.104, (*b*) ICES square 46E9: growth rate = 0.104, (*c*) ICES square 45F1: growth rate = 0.102, (*d*) ICES square 42F2: growth rate = 0.096, (*e*) ICES square 43 E1: growth rate = 0.125, (*f*) ICES square 36E6: growth rate = 0.132.

Age (years)
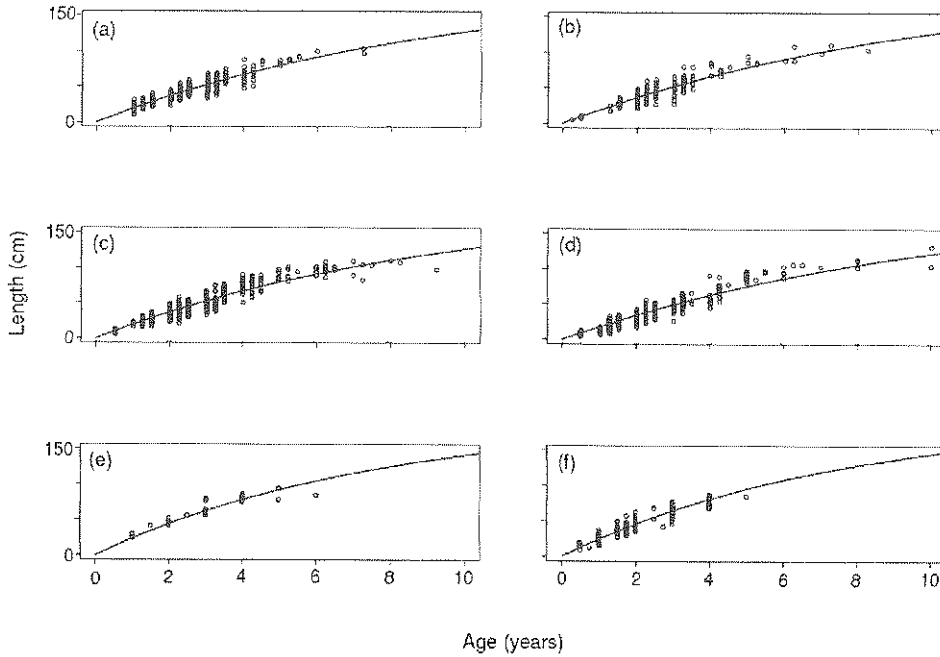
Fig. 4. Fitted growth rates showing (*a*) fitted values of g_x in cells where data is available and (*b*) growth rates for the whole domain with missing data infilled using correlation with temperature and location.

nile and adult segments, we assumed that the background annual mortality rate is a universal function of length (Fig. 6), discussed in detail for the North Sea by Heath et al. (2003) and which we assume applies equally to the other assessment areas.

Individuals who are large enough to settle but cannot do so because the cell they occupy has no suitable ground are subject to the mortality rate appropriate to a settle fish of the same size multiplied by a factor that increases exponentially with length (Appendix A, eq. A37), thus ensuring that such individuals survive only briefly.

Relatively little information is available about mortality rates in larvae and pelagic juveniles. Early attempts to match data with the model described here using spatially uniform pelagic mortality rates were unsuccessful. We thus assume

that the pelagic mortality rate $(\delta^P_{x,t})$ is independent of length, but shows spatio-temporal variation driven by local average temperature $(\overline{T}_{x,t})$ and time (Y, years). For each of the four assessment regions (R) we write

$$(6) \qquad \delta^P_{x,t} = \delta^{PR}_0 + \delta^{PR}_T \, \overline{T}_{x,t} + \delta^{PR}_Y \, Y$$

and regard the parameters $(\delta^{PR}_0, \delta^{PR}_T, \text{ and } \delta^{PR}_Y)$ as free-fitting parameters.

*Fishing mortality*

We assume the time, space, and size dependence of the fishing mortality rate (δ^S_{FL}) can be decomposed into a time-independent length selectivity (C_L) and a year- (y) and assessment region (R)-dependent nominal mortality rate F^R_y, thus

Fig. 5. (a) The proportion mature at length, taken from International Council for the Exploration of the Sea (ICES) estimates of proportion mature at age for the North Sea using a global age–length key (see Appendix A). (b) Proportion mature at age curves for ICES imnd region.
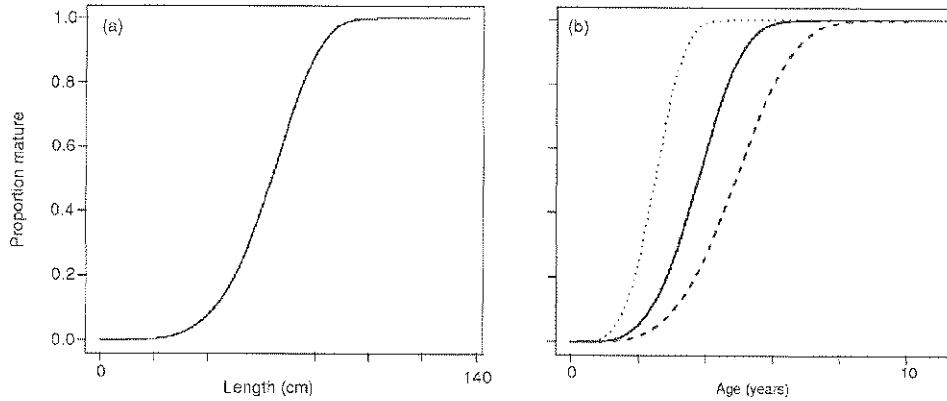
Fig. 6. Annual natural mortality at length for settled fish.
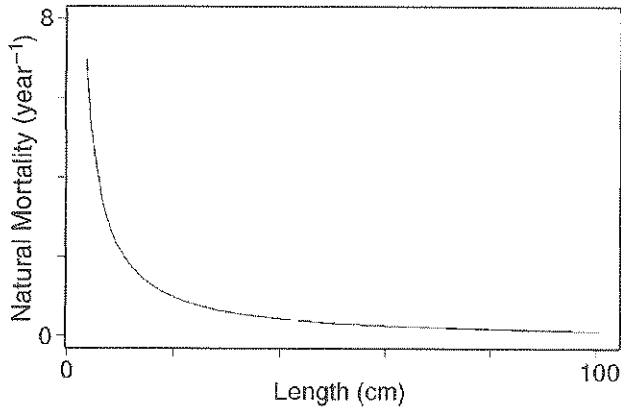
$$(7) \quad \delta_F^S = C_L F_y^R$$

We calculated the age-dependent equivalents of these quantities for each region using the methodology of Cook (1998). We then averaged over regions to obtain an overall age-selectivity, which we transformed to a length selectivity (Fig. 7a) using the global age–length key. We then recalculated the nominal yearly mortality rates by region, so as to match the observed mortality rates as closely as possible. Finally, we smoothed the resulting time series using the R routine supsmu (Friedman 1984a, 1984b). The final results of this process are shown (Fig. 7b).

Carrying capacity

In this model, density-dependent population control is provided by mortality enhancement, which acts if settlement, transport, or somatic growth causes the biomass of settled cod in a given cell to exceed its carrying capacity (defined here as the maximum population density that a particular habitat can support through food supply, refuge for predators, or predator types). To facilitate intercell comparisons, we define cell carrying capacity $k_{x,t}$ as the product of a biomass carrying capacity per unit area (K_x) and the area of bottom that lies between 25 and 200 m (U_x), thus

$$(8) \quad k_{x,t} = K_{x,t} U_x$$

We assume that K_x is linearly related to the local average temperature $(\bar{T}_{x,y})$ and the year (y) thus

$$(9) \quad K_{x,t} = K_0^R + K_T^R \bar{T}_{x,t} + K_Y^R Y$$

where the (region-dependent) coefficients K_0^R, K_T^R, and K_Y^R are regarded as free-fitting parameters.

If the local settled biomass density $(W_{x,t})$ exceeds $k_{x,t}$, all settled individuals are subject to a (length-dependent) additional mortality rate $(\delta_K^S(L))$, which we assume to be proportional to the excess of settled biomass over carrying capacity. For an individual of length L, the additional mortality is assumed to be proportional to its background mortality rate $(\delta_N^S(L))$, so we write

$$(10) \quad \delta_K^S(L) = \begin{cases} \delta_N^S(L)(W_{x,t} - k_x)/k_x & \text{if } W_{x,t} > k_x \\ 0 & \text{otherwise} \end{cases}$$

We calculate the settled biomass by assuming that an individual's weight is proportional to the cube of its length, with a fixed constant of proportionality W_0.

Spawning and fecundity

We assume that the population has a 1:1 sex ratio and that female fish spawn continually between February and April. Eggs are assumed to be released in the cell that is currently occupied by the female concerned. To determine the fecundity of females in each length class, we calculate the equivalent biomass from the global weight–length relation and then use the allometric relation between weight and length given by Marteinsdottir and Begg (2002).

**Movement, mixing, and the physical environment**

Physical environment

The physical environment of the model consists of temperature fields taken from the statistical model reported by Heath et al. (2003), flow fields calculated using a statistical characterization (SNAC; Logemann et al. 2004) of output from the Hamburg Shelf Ocean Model (HAMSOM; Harms et al. 2000), and bathymetry from the National Oceano-

Fig. 7. Fishing mortality showing (*a*) length selectivity (C_L) (Heath et al. (2003)) and (*b*) overall fishing mortality rate F_y^R as a function of year.
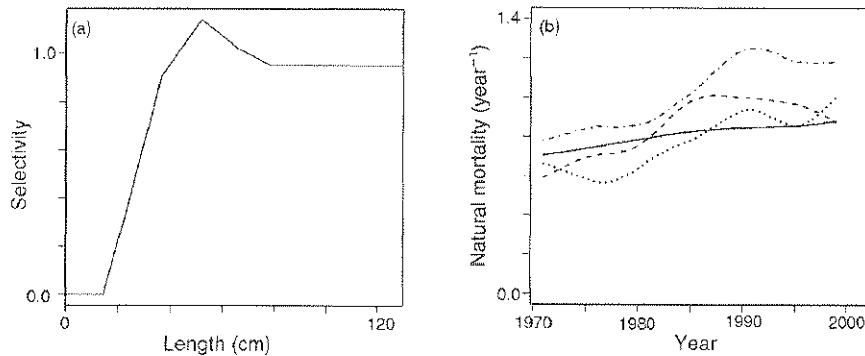
Fig. 8. Surface flows (*a*) and temperature (*b*) in March 1991. Flow fields are produced by SNAC (Logemann et al. 2004) and growth rates are selected from the range used in the model. In panel *b*, the dashed curve is inferred using the slowest growth rate, the solid curve is inferred using the median growth rate, and the dotted curve is inferred using the fastest growth rate.
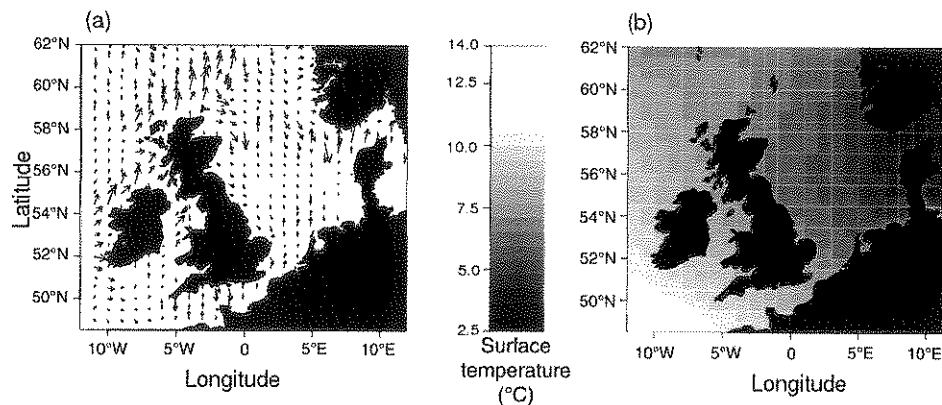
graphic and Atmospheric Administration (http://oceanservice. noaa.gov). The SNAC characterization uses air pressure measurements at eight weather stations to produce daily mean flow rates at 10 depth layers (an example is shown in Fig. 8*a*).

Following the methodology of Gurney et al. (2001), the transfer matrices that define the relocation of eggs, larvae, pelagic juveniles, and settled individuals at biweekly intervals are determined from the SNAC output by tracking an ensemble of 100 particles started from the centre of each cell and assumed to move at a constant depth. For each particle, this deterministic velocity component is supplemented by a random velocity calculated to represent diffusive dispersal with a fixed diffusion coefficient. At the end of the movement period, the number of particles that have relocated to a given cell is counted and used to define the relocation probability.

Movement of eggs, larvae, and pelagic juveniles

All pelagic stages are assumed to be passive passengers on the prevailing currents, and as a modelling approximation, we further assume that each life-history segment is located at a fixed depth. Following Heath et al. (2003), we take the fixed depth for eggs as 6.3 m, that for presettlement juveniles as 25 m, and that for juveniles attempting to settle (i.e., with length >3.5 cm) as 70% of the local bottom depth.

In addition to the deterministic velocity component calculated from SNAC output, we also assume that each individual has a random component equivalent to a diffusion coefficient of 100 m²·s⁻¹.

Movement of settled individuals

Despite extensive tagging studies (e.g., Robichaud and Rose 2001, 2004), we know little about the rules that govern the movements of settled individuals. We shall thus test a series of hypotheses by fitting model variants to historical data on cod abundance. One group of hypotheses concerns the year-round movement of both adults and settled juveniles, namely

1: Settled individuals remain where they settle.
2: Settled individuals diffuse but have no net deterministic movement.
3: Settled individuals move with the current at 1 m above the bottom and diffuse.

A second group of hypotheses concerns movements of adults prior to the spawning season, namely
U: Prior to spawning, adults remain unmoved.
A: Prior to spawning, adults return to the nearest of a set of spawning areas.

To define a complete movement model for settled individuals, we combine hypotheses from these two groups. Thus for example, A2 designates a model in which all settled indi-

Fig. 9. International Council for the Exploration of the Sea (ICES) estimates of spawning stock biomass (SSB) by region. (*a*) North Sea, (*b*) West Coast (*c*) Celtic Sea, (*d*) Irish Sea. Lines show the smoothed trend through the data to which we fit our models.
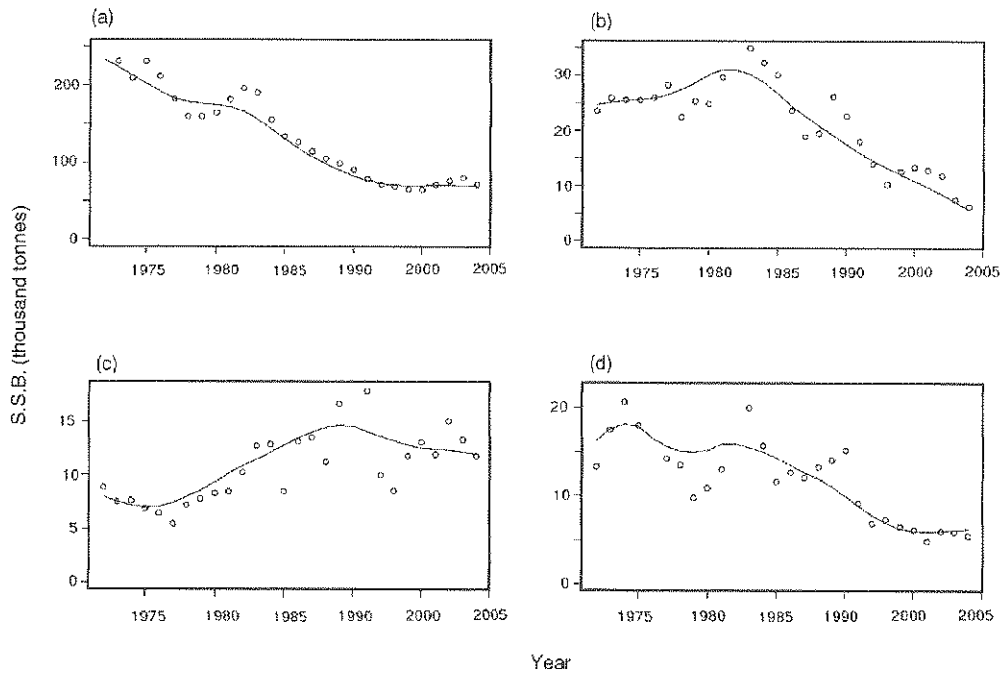
viduals diffuse continuously, and prior to the start of the spawning season adult individuals return instantaneously to the nearest of a set of spawning areas and thereafter continue to diffuse in the normal way. Rather than all returning to a point, the individuals return to a region defined by a tent distribution (i.e., the rotation of a triangular distribution), whose centre and width we regard as free-fitting parameters.

Determining unknown parameters by optimization

Numerical optimization

The model described above contains a number of fixed parameters whose value can be estimated from independent data in the literature. The values for these parameters and the sources from which they are obtained are given in Appendix A.

However, there is also a group of parameters for which no independent data exists. In all model variants, this group includes the region-dependent parameters (δ_0^{PR}, δ_T^{PR}, and δ_Y^{PR}), which define the relationship among temperature, time, and the mortality rate for larvae and unsettled juveniles, respectively. It also always includes region-dependent parameters (K_0^R, K_T^R, and K_Y^R) which determine the relation between the same predictor variables, respectively, and cell carrying capacity. Since the model has four regions, this implies a total of 24 free-fitting parameters concerned with mortality and carrying capacity.

In addition, for the A-series of models (i.e., models with aggregated spawning), we assume that there are six areas where individuals who are about to spawn will aggregate. The position and size of these areas are also regarded as unknowns.

We obtain values for the set of unknown parameters for any given model by fitting to a test data set (see below) comprising smoothed trends in total spawning stock biomass (SSB) for each assessment region over the period 1970–2000 and a decadal average, cell-resolution, spatial distribution of SSB for the period 1990–2000. We optimize the fitting parameter set to fit the model output to this data using the downhill simplex algorithm (Press et al. 1989) with bootstrap restarting (Wood 2001). We optimized against an objective function consisting of 80% of the spatial error and 20% of the trend error, provided that the trend error was less than 1% but rising nonlinearly with trend error where trend error exceeded 1%. We thus, in effect, treated the trend data as a constraint that all reasonable models must be able to reproduce, leaving the more detailed spatial data to perform the final discrimination between plausible models. To reduce the effect of the small number of outlying points, we calculated individual error contributions using absolute rather than square error.

The test data set

The first element of our test data set is the total SSB for each of the four assessment regions: North Sea (ICES 2001*a*, 2002), West Coast (ICES 2001*a*), Celtic Sea, and Irish Sea (ICES 2001*b*). We show the 30-year time series and the smoothed equivalent to which we fit the model (Fig. 9).

The second element of our test data set is the spatial distribution of SSB (Fig. 10). This shows the relative distribution of SSB for the first quarter of the year, determined from data gathered as part of the IBTS and averaged over every year from 1991 to 1998. The raw data from which we worked was gathered under a number of national programs using different gears and protocols.

We could find little reliable, independent data on the catch efficiencies of the gears used, and there was insufficient

Fig. 10. (*a*) Spatial distribution of spawning stock biomass averaged over 1991–1998, inferred from data from the International Bottom Trawl Surveys, reanalysed to harmonize results from disparate sampling gears, and renormalized to enforce consistent regional estimates. Values given are the percentage of total biomass in each model cell. (*b*) The number of hours spent surveying each cell in the 8-year period.
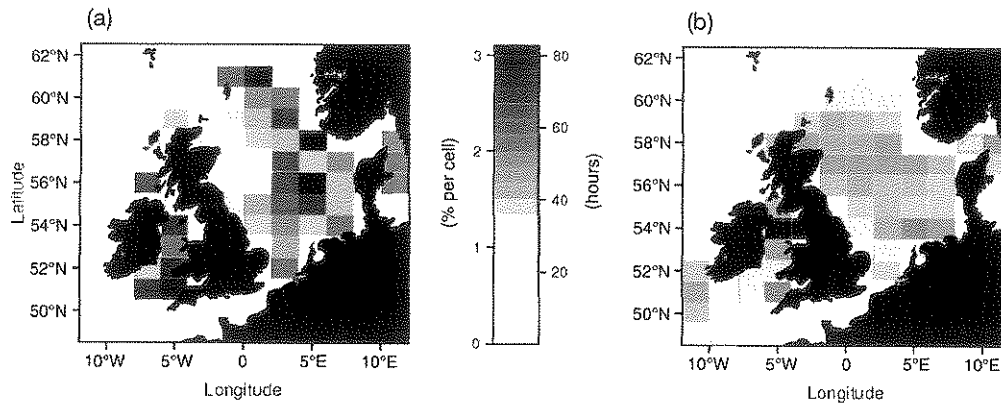
overlap for the surveys to be compared by examining contemporaneous catches in regions of overlap. We were thus forced to take a rather circuitous route from the survey data to the spatial density estimates required to test our model. We first estimated a set of gear- and length-specific catchability coefficients, which minimized the difference between the regional age abundances implied by the IBTS data and the regional age abundances estimated by ICES. Given these catchability coefficients, we then estimated the SSB in each cell in the first quarter of each year and used these estimates to calculate the relative distribution for that year. These relative distributions were averaged over years 1991–1998. This process is described in fuller mathematical detail in Appendix B.

Movement of settled fish — testing hypotheses

We now seek to differentiate among the six hypotheses about the movements of settled individuals set out above. To do this we fit the model to the historical data set discussed in the previous section and compare the best-attainable fits. For comparison purposes, we also fit a further model variant in which no transport of any kind occurs, so the population of each cell is an autonomous unit.

We show the overall quality of the best fit obtainable from these seven models (Table 1) and also show representative examples of the predicted spatial distributions (Figs. 11 and 12). We see that while the uncoupled assemblage of autonomous populations can fit the trend data, within our stipulated 1%, its best attempt at fitting the observed spatial distribution has nearly five times as much spatial error as the best-performing model variant.

The variants with unaggregated spawning, while again fitting the trend to the stipulated accuracy, have spatial errors that are more than twice that of the best-performing variant. Examination of Fig. 11 shows that this large spatial error is indicative of predicted relative spatial distributions of SSB, which place a considerably higher proportion of the population in the southern half of the North Sea and the English Channel than is observed.

Table 1. Minimized errors for model variants.

Spawning	Movement*	Error		
		Spatial	Trend	Total
No transport		141	1	113
Unaggregated	1	73.1	0.99	58.7
	2	76.2	1	61.1
	3	58.2	1	46.7
Aggregated	1	38.5	1	31.0
	2	47.4	1	38.1
	3	28.6	0.99	23.1

Note: Spatial errors are proportional squared errors of the average catch averaged over the cells by the number of hours of surveying in each cell. Trend errors are proportional squared errors of the average spawning stock biomass in each region averaged over the number of data points. The total error is the sum of 80% of the spatial error and 20% of the trend error. All errors are multiplied by 100.
*1, none; 2, diffusive; 3, advective + diffusive.

By comparison, all the model variants with aggregated spawning show low spatial errors, with predicted relative distributions with many of the key features of that which is observed. The best performance comes from the variant with advective movement, and although the quantitative difference in fit quality is not large, we can see patently unrealistic features in the distributions predicted by the other two variants — in both cases the English Channel population is considerably overestimated, and the diffusive variant also places an unrealistic population mass in the central southern North Sea.

We conclude that a spatial demographic model is essential to understanding the population dynamics of cod in the waters around the UK, that aggregated spawning is essential to a qualitatively correct prediction of the spatial distribution of spawning stock, and that long-term advective movement of settled individuals is primarily the result of net transport by local bottom currents.

The best-fit model

We now discuss in more detail the model configuration that provides the best fit to our test data set. We show the best-fit values of the region-specific parameters (Table 2),

Fig. 11. Comparison of survey data with the predictions of the three unaggregated spawning model variants for the first quarter of 1995: (*a*) survey data, (*b*) predictions under hypothesis U1, (*c*) predictions under hypothesis U2, (*d*) predictions under hypothesis U3. (See also Table 1.)
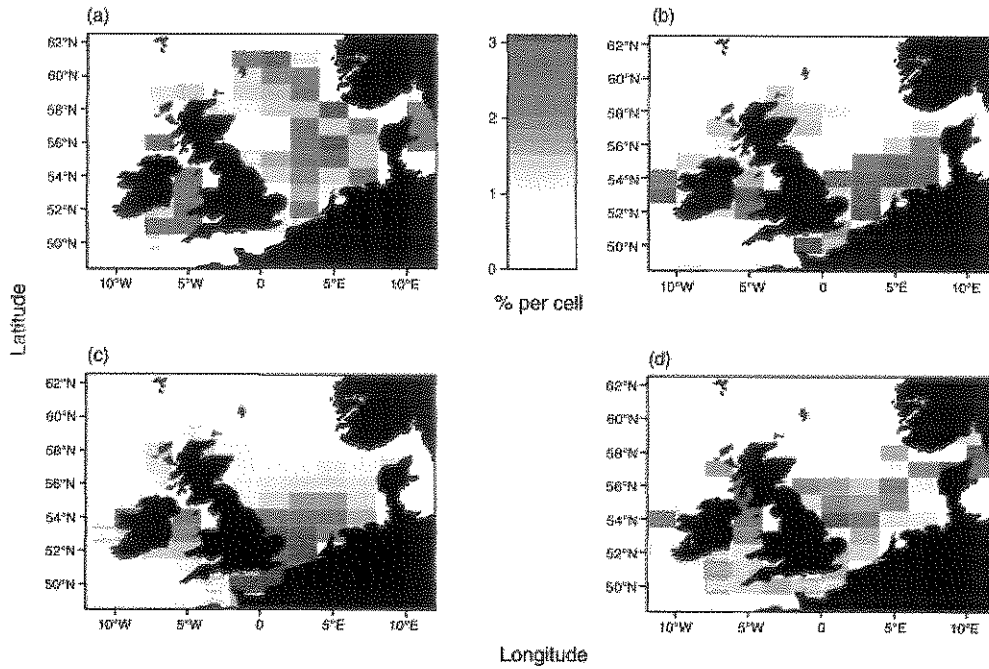
Fig. 12. Comparison of survey data with the predictions of the three aggregated spawning model variants for the first quarter of 1995: (*a*) survey data, (*b*) predictions under hypothesis A1, (*c*) predictions under hypothesis A2, (*d*) predictions under hypothesis A3. (See also Table 1.)
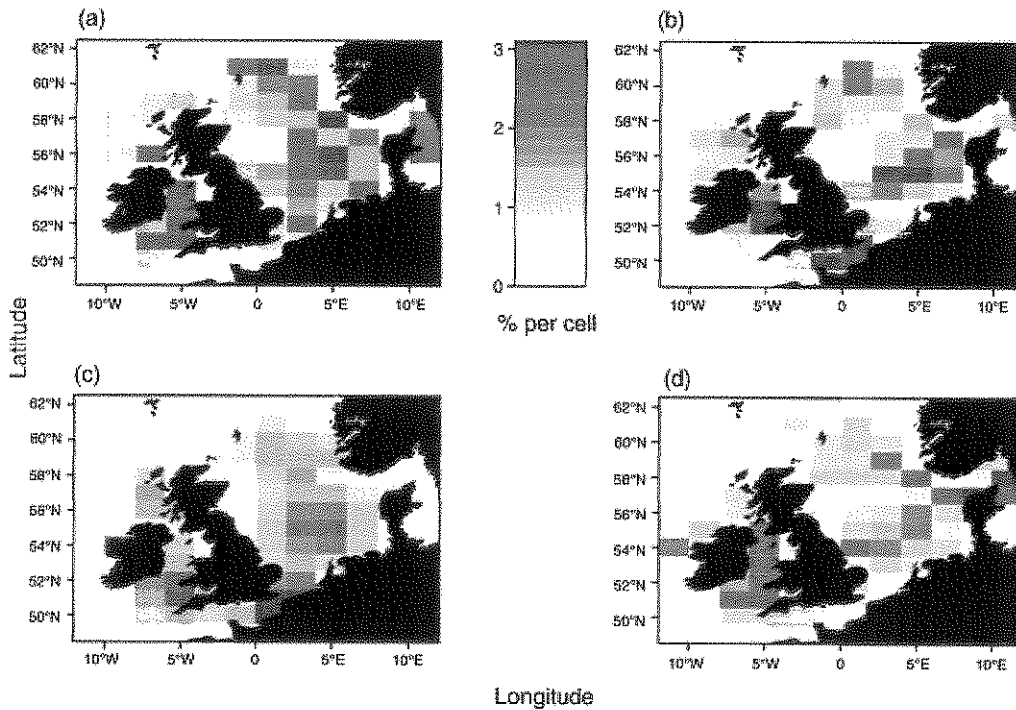
Table 2. Regional parameters for best-fit model.

Region	Carrying capacity (t·km^{-2})			Pelagic mortality (days^{-1})		
	Constant	Temperature	Year	Constant	Temperature	Year
North Sea	1.79	0.0002	−0.000 02	0.095	0.000 017	0.000 094
West Coast	−0.38	0.187	0	0.32	−0.000 14	0.003 3
Celtic Sea	0	0	0.01	0.026	−0.002 4	0.005
Irish Sea	1.87	0	0	0.26	0.007	0.005

which determine the spatial distribution of carrying capacity and larval and juvenile mortality. We see that carrying capacity decreases with time in the North Sea and increases with time in the other three regions, with the most rapid increase occurring in the Celtic Sea. We also note that carrying capacity increases with temperature everywhere except the Irish Sea. Pelagic mortality increases with time everywhere and increases with temperature in the North Sea and the Irish Sea.

We show the spatial distributions of pelagic mortality and carrying capacity calculated from the parameters in Table 2 for the year 2005 (Fig. 13). Pelagic mortality is lowest in the North Sea and highest in the West Coast and Irish Sea areas. Specific carrying capacity is highest in the North Sea and around the north coast of the UK, but is low in the Celtic Sea.

Our best-fit model postulates that immediately prior to the spawning season, the adults who will spawn that year are gathered into six relatively small regions. Each individual goes to the nearest aggregation centre; we show the boundaries of the gathering areas, the centres of the aggregation regions, and the density distribution of spawners immediately after gathering (Fig. 14a).

Immediately after being gathered into the distribution shown (Fig. 14), the adults begin to move again in conformance with the normal movement rules. Eggs are thus deposited over the region through which the spawners move during the spawning season. To illustrate this spawning distribution, we show the average density of adult individuals over the spawning season (Fig. 14b).

We see that our best-fit model predicts a strong area of spawning activity in the South Irish Sea and the Northeast Celtic Sea and a crescent of activity running in an arc from the central-east coast of England across to the Skagarrak and thence north along the southern edge of the Norwegian Trench.

Comparing the predictions of our best-fit model with observations (Fig. 14c) shows good qualitative agreement over most of the domain. In the North Celtic and South Irish seas, we predict locally strong spawning activity in regions where current surveys provide no positive evidence of its existence. Since the white areas in the figure indicate lack of data rather than zero findings, this must be seen as indicating an area where more data need to be brought into the testing process rather than a current indicator of model falsification.

Long-term effects of fishery closures

In this section, we used the best-fit model reported in this paper to explore the effects of a variety of fishing management policies for the North Sea. We first extended our model description to include the best current estimate of the distri-

bution of fishing effort. Indices of international effort could not be obtained for all of the fleets fishing the North Sea cod because of the lack of an agreed data source. Therefore, it was assumed that the spatial pattern of the catch per unit effort (CPUE) of cod at ages 2 and older, recorded by the ICES IBTS for each statistical rectangle, is representative of the annual spatial distribution of CPUE resulting from commercial fishing (STECF 2003). A proxy for the spatial distribution of international effort was calculated from the ration of international commercial landings and the IBTS CPUE series averaged over the years 1999–2002. The spatial distribution of the international landings data was assumed to be representative and unbiased. An unbiased estimate of the absolute level of total landings was not essential to the model results, only the scale relative to other areas. Bias and therefore model error would be introduced by non-uniform spatial distributions of unrecorded removals resulting from discarding or under-reporting. We then refit the model to our test data set reweighted to emphasise the period 1990–2000.

We generated a set of hydrodynamic driving functions for the period 2004–2020 by cyclic repetitions of the years 1994–2004 inclusive and produced temperature-driving functions by assuming that the spatio-temporal temperature distribution remained at that observed in 1999.

We then ran the model forward from 2001 to 2020 under five scenarios: (1) fishing effort and distribution remains constant, (2) the 2001 closures (Fig. 15) remain in force permanently, (3) the Scientific, Technical and Economic Committee for Fisheries (STECF) closures (Fig. 15) remain in force permanently, (4) the northeast English coastal fishery is closed permanently, (5) all fishing effort is removed from the North Sea. For each scenario (except the first and last) we examine two variants. In variant (a) we assume that fishing effort from the closed areas is redistributed over the remaining open area in proportion to existing CPUE, while in variant (b) we assume that displaced effort is removed from the fishery.

We show (Table 3) the predicted total North Sea SSB at 5-year intervals over the prediction period. Without any change in regulatory policy, the continuation of recent trends (scenario 1) leads to the SSB being halved by 2020. By (extreme) contrast, the entire removal of fishing effort from 2001 onwards results in a recovery to an SSB of 272 thousand tonnes by 2005, with the population reaching its carrying capacity by 2015 and thereafter being carried downwards by the continuing downward trend in carrying capacity. All the closure policies except four produce major improvements, but only those in which effort is removed rather than redistributed result in serious progress being made in moving SSB towards a substantial fraction of carrying capacity.

Fig. 13. (*a*) Carrying capacity distribution in thousands of tonnes per cell calculated for 2005. (*b*) Contemporaneous pelagic mortality rate (day^{-1}).
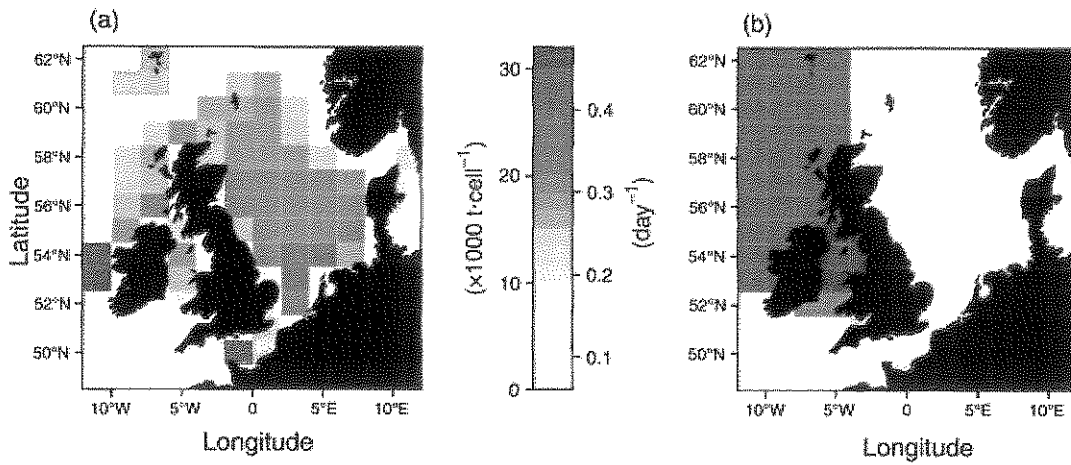

Fig. 14. (*a*) The predicted aggregated distribution of spawners immediately prior to the 1995 spawning season. The boundaries of each gathering region are shown in black, with the centre of the aggregation region marked with a red zone. (*b*) The predicted average distribution of spawners over the 1995 spawning season. (*c*) The observed distribution of spawning fish. Dark grey indicates cells containing currently active spawning areas; white indicates no data. Derived from data presented by Wright et al. (2003), Heath et al. (2003), and C.J. Fox (Centre for Environment, Fisheries & Aquaculture Science (Cefas), Lowestolt Laboratory, Palcefield Road, Lowestoft, Suffolk, NR33 OHT, UK, personal communication).
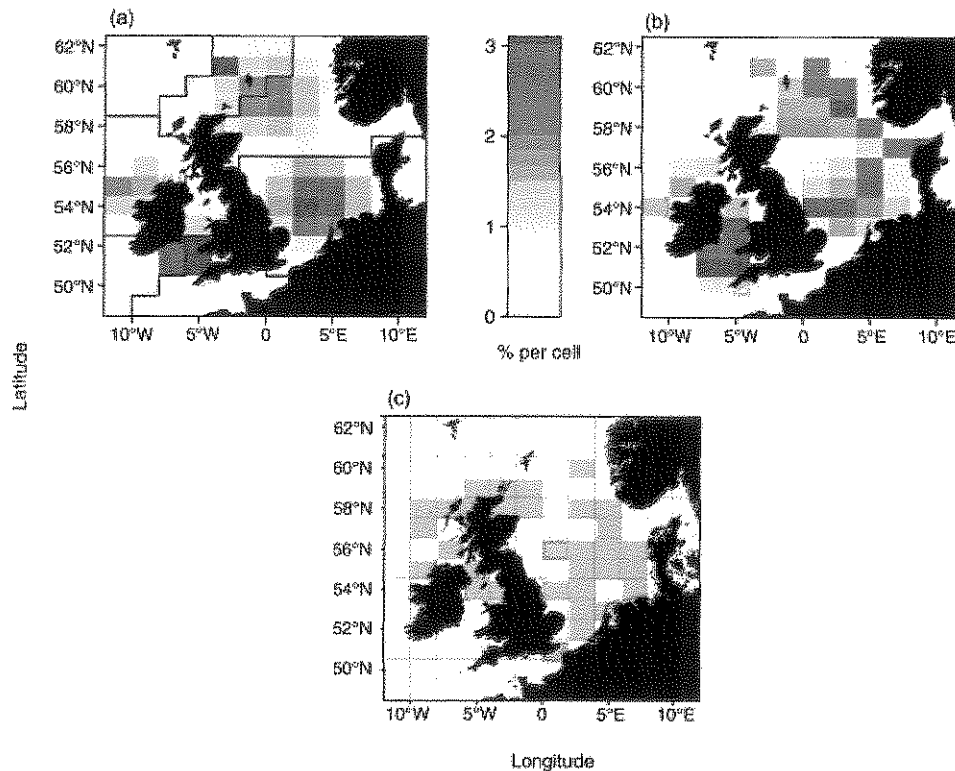
We show (Fig. 15) the relative distribution of SSB predicted in 2015. Comparing Fig. 12*a* with Fig. 12*d*, we see that with no change in regulatory policy, the North Sea spawning stock appears to have moved south and to be primarily concentrated in an area between the central-southern English coast and the Skagarak. Interestingly, the two closure policies that produce important population enhancement do so by reinforcing this population concentration, which we note does not lie to any large degree within the areas from which fishing effort is excluded. This emphasises the need

Fig. 15. The predicted spatial distribution of spawning stock biomass in 2015 under various scenarios: (*a*) scenario 1, (*b*) scenario 2*b*, (*c*) scenario 3*b*, (*d*) scenario 4*b*. The areas closed to fishing in each case are shown outlined with a solid black line. (See also Table 3.)
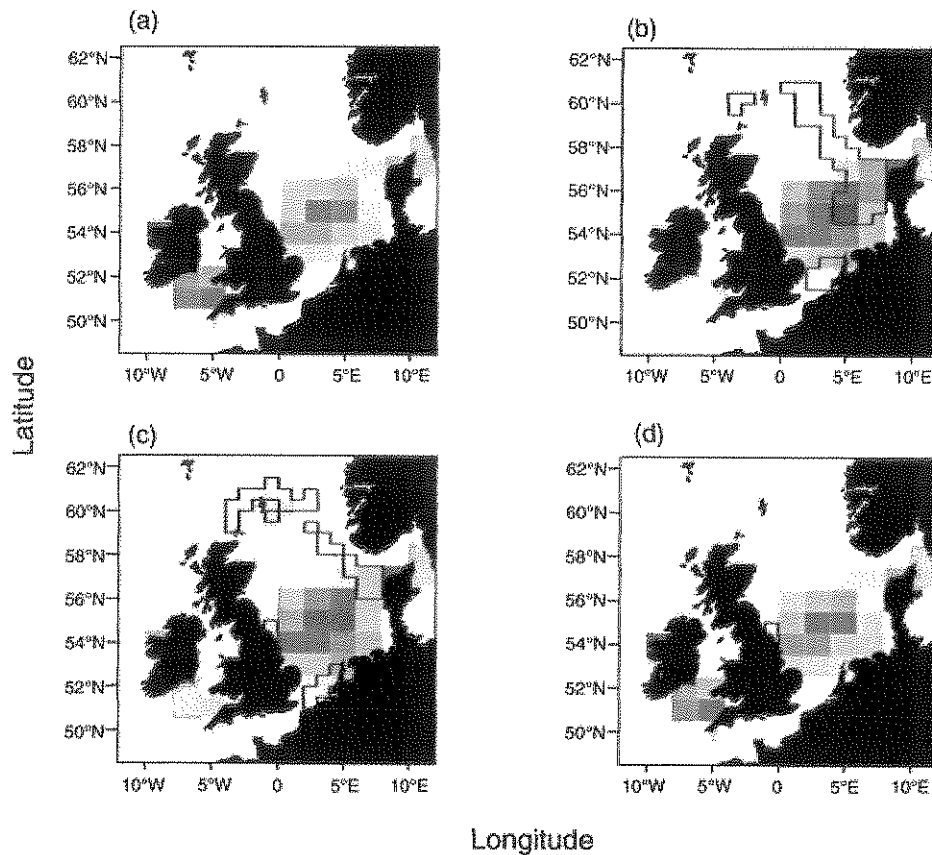
Table 3. Forward projections of total North Sea spawning stock biomass (in thousands of tonnes) under scenarios 1–5 with variants (*a* = effort redistributed; *b* = effort removed) for scenarios 2–4.

Year	Scenario–variant							
	1	2a	2b	3a	3b	4a	4b	5
2001	47	47	47	47	47	47	47	47
2005	39	75	91	53	67	43	43	272
2010	31	66	94	46	64	33	34	360
2015	22	63	102	38	59	25	25	458
2020	22	68	112	39	64	25	25	401

for spatial models in designing and evaluating possible closure policies.

Discussion

Simulating the multi-annual dynamics of spatial demography for a high fecundity species such as cod represents a considerable challenge. The difficulties arise principally from the requirement to dynamically close the life cycle, which spans the pelagic and demersal environment and six orders of magnitude in body weight. The dispersal, growth, and mortality of the pelagic early life stages are intimately linked to oceanographic conditions, while the settled juve-

niles and adults have very much lower specific growth and mortality rates and undertake directed migrations, but are also subjected to a spatially and temporally variable, size-selective, external predation by the fisheries. In addition, the processes leading to variability in early-life survival are poorly understood, though they seem to be correlated with temperature and aspects of plankton abundance (O'Brien et al. 2000; Beaugrand et al. 2003) and little is known of the motivations for directed migrations in juveniles and adults.

To model the cod stocks, we needed to simulate long-term patterns in the multi-annual cohort populations of sparsely distributed adults, combined with the dynamics of annual pulses of densely distributed eggs and larvae. The relative merits of different schemes for simulating spatial demography in structured populations are well documented (Gurney and Nisbet 1998). In general, individual- or meta-individual-based Lagrangian systems are appropriate for short-term simulations (relative to the generation time) of sparsely distributed individuals. Eulerian methods combining biological development with advection–diffusion algorithms are more appropriate for long-term studies of dense populations, where the distribution in time and space approximates to a continuous function. However, the numerics of continuous-time solutions to the Eulerian approach are notoriously difficult. Hence we adapted the discrete time approach of Gurney et al. (2001), originally devised to model the ocean basin de-

Table 4. List of possible processes leading to compensatory effects on survival, together with possible schemes for their representation in a model system.

Process	Manifestation
1. Competition for refuge or territory	Exclusion of late-arriving individuals by the presence of conspecifics in a particular habitat; consequent mortality
2. Necessity to form schools for protection from predators	School sizes increase with population abundance, such that individual members obtain less food with consequent effects on growth rates
3. Competition for food; some types of parasitism of larvae or juveniles	Inverse relationship between local abundance of conspecifics in a given size range and individual growth rates
4. Cannibalism	Size-specific mortality rate positively related to the abundance of larger conspecifics in the vicinity
5. Attraction of predators to local abundances of the target species; some types of disease	For a given size range of individuals, size-specific mortality rate positively related to local abundance of conspecifics

mography of a planktonic copepod. In addition to resolving the numerical problems associated with other Eulerian methods, this also provides important gains in computational efficiency, enabling automatic optimization of less well-known parameters to enable the model to conform with established observations.

Recruitment processes

The balance between recruitment (young-of-the-year abundance) and mortality dictates the demographic distribution and trends in abundance of the settled population of cod. However, representing recruitment in a spatially resolved model is especially difficult. The problem is to determine what proportion of the eggs produced at a given spatial node recruit to all other spatial nodes in the system. Ideally, one would want to fully close the life cycle and explicitly represent the dispersal and survival processes involved. However, since these are almost always poorly understood, previous studies have employed varying degrees of external forcing. For example, Lehodey et al. (2003) developed a spatial model of skipjack tuna (*Katsuwonus pelamis*) population dynamics in the Pacific Ocean. The basin scale population of skipjack tuna was represented by a (horizontally) spatially resolved, age-structured cohort model, which tracked the numbers of individuals at age over space and time (Lehodey 2001). The relative spatial distribution of recruitment, was parameterized from a linked physical–biogeochemical model, but the magnitude of spatially integrated recruitment was an external driving term derived from fishery monitoring and an independent statistical assessment model. In contrast, we have not constrained our model by imposed recruitment as external driving data; neither have we specified a functional relationship between stock and recruitment. Any such relationship is an emergent property of our model, resulting from underlying processes that we have represented explicitly, in particular the pelagic stage mortality rates, carrying capacities of the various regions, and the interaction between spatial patterns of egg production and pelagic stage dispersal and settlement.

Density dependence must play a key role in establishing recruitment, as evidenced by the underlying shape of typical scatterplots of data on spatially aggregated cod recruitment and spawning stock abundance (Beverton and Holt 1957; Ricker 1975). There is no sound evidence to support a case for density dependence during the pelagic phase of cod, but there are reasonable grounds for accepting that the key pro-

cesses act during the transition from pelagic to demersal habitat, referred to here as settlement (Heath and Brander 2001). Table 4 gives a number of hypothetical mechanisms by which survival at settlement may be compromised by increases in spawning population abundance.

These are neither mutually exclusive nor necessarily always operative under all conditions for any given species. Central to all of the hypotheses regarding settlement processes is the concept of carrying capacity. Defining the carrying capacity of the domain is critical for the performance of our model system and is particularly problematic by any independent means. In the Northwest Atlantic, manned submersibles and remotely operated vehicles have been used to observe juvenile cod in the field. These studies seem to indicate that certain sediment types confer a camouflage refuge (Lough et al. 1989; Gregory and Anderson 1997), while other sediment types leave the fish exposed to detection by predators. Anecdotal information from these studies suggests that recently settled fish may also utilize weed mats and boulders for refuge. However, analysis of survey abundances of juvenile cod in relation to habitat categories does not necessarily provide information on carrying capacity, since the extent to which the available capacity is occupied at each sampling location remains unknown.

We adopted a simple "self-thinning" representation of density dependence in our model (process 1, 4, or 5 in Table 4), based on the total sustainable biomass density of cod at a given location. We regarded the settlement habitat as being defined simply on the basis of depth and hypothesized that the area-specific carrying capacity might vary between regions and linearly with temperature and time and optimized the parameter values to maximize the model fit to observations of SSB. The fitted parameters for the optimal model indicate an average carrying capacity of approximately 2000 $kg \cdot km^{-2}$ in the North Sea, West Scotland, and Irish Sea regions, which is equivalent to about 0.2 g $C \cdot m^{-2}$ and represents an annual food demand of 1 g $C \cdot m^{-2} \cdot year^{-2}$. According to calculations by Heath (2005), this represents approximately 6% of the total food demand of fish in the North Sea during the 1970s. Carrying capacity was estimated to be markedly lower in the Celtic Sea and increasing over time. Elsewhere, the optimum carrying capacity was estimated to be stable over time.

Since almost nothing is known about spatial and temporal patterns of pelagic stage mortality in cod, we hypothesized that like the carrying capacity, these too might vary between

regions and with temperature and over time. The optimized mortality rates varied between regions and, in contrast with the carrying capacity, with temperature and time. In all regions, the results implied that pelagic mortality was increasing over time; in the North Sea and Irish Sea, it seemed to increase with temperature. Since average temperature in European shelf seas has had an increasing trend since 1970, the time and temperature effects are effectively compounded. In the North Sea, temperature has increased at a rate of approximately 0.6 °C per decade (Hughes 2004), and the fitted parameters imply a 20% reduction in survival to the onset of settlement per degree rise in temperature (equivalent to 16 years). This result is comparable with the temperature sensitivity inferred by incorporating a temperature term into the standard Ricker stock–recruitment function and fitting to recruitment, spawning biomass, and temperature data from the North Sea as if they were independent observations (O'Brien et al. 2000).

Dispersal and migration

Modelling the dispersal of fish eggs and larvae by particle tracking through simulated hydrodynamic flow fields is a well-established technique (Werner et al. 2001; Mullon et al. 2003; Bartsch and Coombs 2004), and the off-line particle tracking carried out to support our model was consistent with previous studies. The new development here was the conversion of particle-tracking results into transfer matrices as driving data for pelagic dispersal aspects of the cod population model. Gurney et al. (2001) showed that with careful choice of grid cell dimensions and time step, this technique reproduces closely the results from particle tracking, but makes a great gain in computational speed.

The underlying SNAC model provides 30-day moving average data on the most probable residual circulation pattern resulting from a given weather situation. The model computes the horizontal components of the current vectors in a series of layers on a spherical grid with a longitudinal resolution of 0.125° and a latitudinal resolution of 0.25° (approximately 14 km) from statistical relationships with horizontal air pressure gradients around the North Atlantic. The advantage of using SNAC as opposed to a fully three-dimensional hydrodynamic model is that air pressure data are readily available from 1948 onwards, and the corresponding flow fields can be computed at minimal cost. The disadvantage is that the resulting flow fields are smoothed and hence will not reflect peaks of horizontal transport. However, given the much coarser resolution of the transfer matrices used to drive the cod model (110 km), this smoothing should not be a critical issue. We have independently validated the output from SNAC by comparison with a set of 6-month (duration) recording current meter deployments in the northwestern North Sea during 2002 (A. Gallego, unpublished data).

Our main sensitivity analysis of the model focussed on the structural uncertainty surrounding the migration behaviors of juvenile and adult cod. In this, we treated the other major areas of uncertainty (pelagic mortality and the specific carrying capacity of the environment) as free fitting and optimized each structural variant of the model to the established levels, trends, and distributions of SSB. The analysis clearly showed that structural variants of the model that do not re-

cognise two modes of behavior in the adult fish (i.e., (*i*) an active seasonal migration to a set of spatially stable spawning sites followed by (*ii*) a dispersal phase) cannot under any fitting circumstances explain both the abundance and distribution of the spawning stock.

The behavioural details of the best-fitting structural variant of the model are of course only a crude and general caricature of the actual migration behaviour of cod, but they clearly capture an essential element of the behaviour of the majority of fish. In reality, cod migrations are certainly much more complicated. Based on a synthesis of tagging data, Robichaud and Rose (2004) proposed four categories of cod populations according to the extent of migration and spawning site fidelity: "sedentary residents" that exhibit year-round site fidelity, "accurate homers" that return to spawn in a specific area, "inaccurate homers" that return to a broader area around the original spawning site where they were tagged, and "dispersers" that move apparently at random and spawn anywhere within large geographical regions. Genetic studies indicate that homers and especially sedentary residents may also be reproductively isolated from other groups of fish (Ruzzante et al. 2000; Knutsen et al. 2003) and exhibit divergent phenotypic traits (Olsen et al. 2004; Salvanes et al. 2004). Resident populations appear to be most common in coastal areas (Green and Wroblenski 2000; Knutsen et al. 2003; Imsland and Jonsdottir 2003). Tagging results indicate resident populations in some coastal areas of the North Sea, for example around the Shetland Islands (P. Wright, FRS Marine Laboratory, Aberdeen AB11 9DB, Scotland, personal communication) and in the Clyde Sea (Conolly and Officer 2001), and might also be expected in the fjords of the west coast of Scotland. The bulk of cod around the UK appear, however, to be inaccurate homers or dispersers.

Spatial closures

The regime of spatially structured fishery closures or marine protected areas in the North Sea is proposed as a management measure to promote the recovery of cod stocks while minimizing the social and economic impact of other fisheries. Our results clearly show that the effectiveness of this strategy is greatly limited unless the displaced fishing effort is removed completely from the system. Simply displacing the effort to an adjacent, unprotected area substantially limits the effectiveness of the measure. Most importantly though, our models shows that the benefits of a spatial closure scheme may be manifest elsewhere in the region rather than in the immediate vicinity of the closure, thus reinforcing the need for spatial models that adequately represent the dispersal and migrations of the fish. If, as has been suggested by recent genetic studies (Hutchinson et al. 2001), the North Sea comprises a series of substocks, closure of an area containing one substock may completely protect it from exploitation while forcing effort onto a second, making it more vulnerable to exploitation.

thanks go to the people working on the collection of assessment data, tagging data, and sex–maturity age–length keys data at ICES, the Department of Agriculture and Regional Development (DARD, Belfast, Northern Ireland), CEFAS, and FRS, without whom this sort of work would not be possible. Special thanks must go to B. Rackham, D. Maxwell, M. Armstrong, and S. Jennings at CEFAS; C. Needle at FRS; and E. McKenzie at the University of Strathclyde for their help at various stages of the project.

References

Bartsch, J., and Coombs, S. 2004. An individual-based model of the early lifehistory of mackerel *Scomber sombrus* in the eastern N. Atlantic simulating transport, growth and mortality. Fish. Oceanogr. **13**: 365–379.

Beaugrand, G., Brander, K., Lindley, J., Souissi, S., and Reid, P. 2003. Plankton effect on cod recruitment in the North Sea. Nature (London), **426**: 661–664.

Beverton, R., and Holt, S. 1957. On the dynamics of exploited fish populations. Fish. Inv. Lond. Ser. **19**: 1–533.

Brander, K. 1994. Spawning and life history information for North Atlantic cod stocks. ICES Coop. Res. Rep. 205.

Brander, K., and Mohn, R. 2004. Effect of the North Atlantic Oscillation on recruitment of Atlantic cod (*Gadus morhua*). Can. J. Fish. Aquat. Sci. **61**(9): 1558–1564.

Child, A. 1988. Population genetics of cod (*Gadus morhua* (L)), haddock (*Melanogrammus eaglefinus* (L)), whiting (*Merlangius merlangus* (L)) and saithe (*Pollachius virens* (L)). Ministry of Agriculture, Fisheries and Food (MAFF), Essex, U.K. MAFF Fish. Res. Tech. Rep. 87.

Conolly, P., and Officer, R. 2001. The use of tagging data in the formulation of the Irish Sea recovery plan. ICES CM 2001 05.

Cook, R.M. 1998. A sustainability criterion for the exploitation of North Sea cod. ICES J. Mar. Sci. **55**: 1061–1070.

Cook, R.M., Sinclair, A., and Stefansson, G. 1997. Potential collapse of North Sea cod stocks. Nature (London), **385**: 521–522.

Daan, N. 1978. Changes in cod stocks and cod fisheries in the North Sea. Rapp. P.-V. Reun. Cons. Int. Explor. Mer, **172**: 39–58.

Fox, C., O'Brien, C., Dickey-Collas, M., and Nash, R. 2000. Patterns in the spawning of cod (*Gadus morhua* L.), sole (*Solea solea* L.), plaice (*Pleuronectes platessa* L.,) in the Irish Sea as determined by generalised additive models. Fish. Oceanogr. **9**: 33–49.

Frank, K., and Brickman, D. 2000. Allee effects and compensatory population dynamics within a stock complex. Can. J. Fish. Aquat. Sci. **57**: 513–517.

Friedman, J. 1984a. SMART user's guide. Stanford University, Stanford, Calif. Tech. Rep. 1.

Friedman, J. 1984b. A variable span scatterplot smoother. Stanford University, Stanford, Calif. Tech. Rep. 5.

Green, J., and Wroblenski, J. 2000. Movement patterns of Atlantic cod in Gilbert Bay, Labrador: evidence for bay residence and spawning site fidelity. J. Mar. Biol. Assoc. U.K. **80**: 1077–1085.

Gregory, R., and Anderson, J. 1997. Substrate selection and use of protective cover by juvenile Atlantic cod *Gadus morhua* in the inshore waters of Newfoundland. Mar. Ecol. Prog. Ser. **146**: 9–20.

Gurney, W., and Nisbet, R. 1998. Ecological dynamics. Oxford University Press, Oxford, UK.

Gurney, W., Speirs, D., Wood, S., Clarke, E., and Heath, M. 2001. Simulating spatially and physiologically structured populations. J. Anim. Ecol. **70**: 881–894.

Harms, I., Heath, M., Bryant, A., Backhaus, J., and Hainbucher, D. 2000. Modelling the Northeast Atlantic circulation: implications for the spring invasion of shelf regions by *Calanus finmarchicus*. ICES J. Mar. Sci. **57**: 1694–1707.

Heath, M. 2005. Changes in the structure and function of the North Sea fish food web. ICES J. Mar. Sci. **62**: 847–868.

Heath, M., and Brander, K. 2001. Workshop on Gadoid Stocks in the North Sea During the 1960's and 1970's. Fourth ICES/GLOBEC Backward-Facing Workshop 1999. ICES Coop. Res. Rep. 244.

Heath, M., MacKenzie, B., Ådlandsvik, B., Backhaus, J., Begg, G., Drysdale, A., Gallego, A., Gibb, F., Gibb, I., Harms, I., Hedger, R., Kjesbu, O., Logemann, K., Marteinsdottir, G., McKenzie, E., Michalsen, K., Nielsen, E., Scott, B., Strugnell, G., Thorsen, A.A., Visser, A., Wehde, H., and Wright, P. 2003. An operational model of the effect of stock structure and spatio-temporal factors on recruitment — final report of the EU-STEREO Project FAIR-CT98-4122. Fish. Res. Serv. Contr. Rep. 10/03.

Hughes, S. 2004. The Scottish ocean climate status report 2002 and 2003. Fisheries Research Services, Aberdeen, UK.

Hutchinson, W.F., Carvalho, G.R., and Rogers, S.I. 2001. Marked genetic structuring in localised spawning populations of cod *Gadus morhua* in the North Sea and adjoining waters as revealed by microsatellites. Mar. Ecol. Prog. Ser. **223**: 251–260.

Hutchinson, W.F., Oosterhout, C., Rogers, S., and Carvalho, G. 2003. Temporal analysis of archived samples indicates marked genetic changes in declining North Sea cod (*Gadus morhua*). Proc. R. Soc. Lond. B Biol. Sci. **270**: 2125–2132.

ICES. 2001a. Report of the Working Group on the assessment of demersal stocks in the North Sea and Skaggerak. ICES CM 2001 ACFM:07.

ICES. 2001b. Report of the Working Group on the assessment of Southern Shelf demersal stocks. ICES CM 2001 ACFM:05.

ICES. 2002. Report of the Working Group on the assessment of demersal stocks in the North Sea and Skagerrak. ICES CM 2002/ACFM: 01.

ICES. 2003. Report of the ICES Advisory Committee on fishery management. 2002. ICES Coop. Res. Rep.

Imsland, A., and Jonsdottir, O. 2003. Linking population genetics and growth properties of Atlantic cod. Rev. Fish Biol. Fish. **13**: 1–26.

Jamieson, A., and Thompson, D. 1972. Blood proteins in North Sea cod (*Gadus morhua* L.). *In* Proceedings of the 12th European Conference on Animal Blood Groups and Biochemical Polymorphism. *Edited by* G. Kovacs and M. Papp. Junk, The Hague, Netherlands. pp. 585–591.

Knutsen, H., Jorde, P., Andre, C., and Stenseth, N. 2003. Fine-scaled geographical population structuring in a highly mobile marine species: the Atlantic cod. Mol. Ecol. **12**: 385–394.

Kurlanski, M. 1999. Cod. A biography of the fish that changed the world. Vintage Press, London, UK.

Lehodey, P. 2001. The pelagic ecosystem of the tropical Pacific Ocean: dynamic spatial modelling and biological consequences of ENSO. Prog. Oceanogr. **49**: 439–468.

Lehodey, P., Chai, F., and Hampton, J. 2003. Modelling climate-related variability of tuna populations from a coupled ocean–biogeochemical-populations dynamics model. Fish. Oceanogr. **12**: 483–494.

Logemann, K., Backhaus, J., and Harms, I. 2004. SNAC: a statistical emulator of the north-east Atlantic circulation. Ocean Modell. **7**: 97–110.

Lough, R., Valentine, P., Potter, D., Auditore, P., Boltz, G., Neilson, J., and Perry, R. 1989. Ecology and distribution of juvenile cod and haddock in relation to sediment type and bottom currents on eastern Georges Bank. Mar. Ecol. Prog. Ser. **56**: 1–12.

Marteinsdottir, G., and Begg, G. 2002. Essential relationships incorporating the influence of age, size and condition on variables

required for estimation of reproductive potential in Atlantic cod *Gadus morhua* stocks. Mar. Ecol. Prog. Ser. **235**: 235–256.

Mullon, C., Freon, P., Parade, C., der Lingen, C.V., and Huggett, J. 2003. From particles to individuals: modelling the early stages of anchovy (*Engaulis capensis/encrasicolus*) in the southern Bengula. Fish. Oceanogr. **12**: 396–406.

O'Brien, C.M., Fox, C.J., Planque, B., and Casey, J. 2000. Climate variability and North Sea cod. Nature (London), **404**: 142.

Olsen, E., Knutsen, H., Gjosaeter, J., Jorde, P., Knutsen, J., and Stenseth, N. 2004. Life-history variation among local populations of Atlantic cod from the Norwegian Skagerrak coast. J. Fish. Biol. **64**: 1725–1730.

Page, F., and Frank, K. 1989. Spawning time and eggs stage duration in Northwest Atlantic haddock (*Melanogrammus aeglefinus*) stocks with emphasis on Georges and Browns bank. Can. J. Fish. Aquat. Sci. **46**(Suppl. 1): 68–81.

Planque, B., and Frédou, T. 1999. Temperature and the recruitment of Atlantic cod (*Gadus morhua*). Can. J. Fish. Aquat. Sci. **56**: 2069–2077.

Press, W.H., Flannery, B.P., Teukolsky, S.A., and Vetterling, W.T. 1989. Numerical recipes in Pascal. The art of scientific computing. Cambridge University Press, Cambridge, UK.

Ricker, W. 1975. Computation and interpretation of biological statistics of fish populations. Bull. Fish. Res. Board Can. 191.

Rijnsdorp, A., and Jaworski, A. 1990. Size-selective mortality in plaice and cod eggs — a new method in the study of egg mortality. J. Conseil, **47**: 256–263.

Robichaud, D., and Rose, G. 2001. Multiyear homing of Atlantic cod to a spawning ground. Can. J. Fish. Aquat. Sci. **58**: 2325–2329.

Robichaud, D., and Rose, G.A. 2004. Migratory behaviour and range in Atlantic cod: inference from a century of tagging. Fish Fish. **5**: 185–214.

Rose, G. 2004. Reconciling overfishing and climate change with stock dynamics of Atlantic cod (*Gadus morhua*) over 500 years. Can. J. Fish. Aquat. Sci. **61**: 1553–1557.

Ruzzante, D., Wroblenski, J., Taggart, C., Smedbol, R., Cook, D., and Goddard, S. 2000. Bay-scale population structure and coastal Atlantic cod in Labrador and Newfoundland. J. Fish Biol. **56**: 408–431.

Salvanes, A., Skjaeraasen, J., and Nilsen, T. 2004. Sub-populations of coastal cod with different behaviour and life-history strategies. Mar. Ecol. Prog. Ser. **267**: 241–251.

Sinclair, M. 1988. Marine populations. An essay on population regulation with speciation. Washington Sea Grant Program, Seattle, Wash.

Speirs, D., Gurney, W., Heath, M., and Wood, S. 2005. Modelling the basin-scale demography of *Calanus finmarchicus* in the North-east Atlantic. Fish. Oceanogr. **14**: 333–358.

Scientific, Technical and Economic Committee for Fisheries (STECF). 2003. Meeting on Cod Assessment and Technical Measures, 28 April – 7 May 2003. *Edited by* H. Ratz. STECF, Brussels, EU.

von Bertalanffy, L. 1957. Quantitative laws in metabolism and growth. Q. Rev. Biol. **32**: 217–232.

Werner, F., Quinlan, J., Lough, G., and Lynch, D. 2001. Spatially explicit individual-based modelling of marine populations: a review of the advances in the 1990's. Sarsia, **86**: 411–421.

West, W.-B. 1970. The spawning biology and fecundity of cod in Scottish waters. Ph.D. thesis, University of Aberdeen, Scotland.

Wood, S. 2001. Minimising model-fitting objectives that contain spurious local minima by bootstrap restarting. Biometrics, **57**: 240–244.

Wright, P., Gibb, F., Gibb, I., Heath, M., and McLay, H. 2003. North Sea cod spawning grounds. Fish. Res. Serv. Internal Rep. 17 03.

Yoneda, M., and Wright, P. 2004. Temporal and spatial variation in reporoductive investment of Atlantic cod, *Gadus morhua*, in the northern North Sea and Scottish west coast. Mar. Ecol. Prog. Ser. **276**: 237–248.

Appendix A. Technical specification of the model.

State variables

Our model is closely related to that used by Speirs et al. (2005) to describe the dynamics of the oceanic copepod *Calanus finmarchicus* in the Northeast Atlantic. It describes a domain from 48.5°N to 62°N and from 12°W to 12°E, divided into cells measuring 1°N × 2°E, each identified by a vector address $x = \{N, E\}$, where N and E respectively represent the latitude and longitude of the cell centre.

We divide the cell population into settled individuals (who are supposed to be located on or near the seabed), unsettled individuals (who are supposed to be in the water column), and eggs (which are supposed to be at the top of the water column). Each of these groupings is regarded as being composed of a sequence of developmental classes, chosen so that promotion from each one to its successor happens at the same instant for all classes in the grouping.

We characterize eggs by the proportion p of the development required to pass from release to hatching, which they have currently achieved, and subdivide the local egg population into development classes of width Δp, each denoted by its upper bounding development, so that the last cell in the sequence has $p = 1$.

We assert that the properties of both unsettled and settled fish are determined by their length (L), which changes according to a von Bertalanffy growth law

$$(A1) \quad \frac{dL}{dt} = \gamma_x(L_\infty - L)$$

To group these individuals so that promotion from one class to another happens at the same instant for all classes, we assume that L_∞ is constant in both space and time and adopt a development index

$$(A2) \quad q \equiv \ln\left(\frac{L_\infty - L_H}{L_\infty - L}\right)$$

where L_H is the length of a newly hatched individual, whose development index is thus 0. We subdivide the settled and unsettled populations into classes of width Δq, each denoted by the value of q at its lower boundary.

Our cells vary in area, so we use cell populations as state variables, thus

$(A3) \quad E_{p,x,t} \equiv$ eggs in class p in cell x at time t

$(A4) \quad J_{q,x,t} \equiv$ unsettled class q individuals

in cell x at time t

$(A5) \quad S_{i,q,x,t} \equiv$ immature settled class q individuals

in cell x at time t

(A6) $A_{m,q,x,t} \equiv$ mature settled class q individuals

in cell x at time t

The physical model

The physical transport of individuals from one cell to another is simulated by updating the system state at a series of times $\{U\}$, separated by the transport update interval Δt. At a transport update, the state of each local population class is changed from that infinitesimally before the update (e.g., $E^-_{p,x,t}$) to that infinitesimally after it (e.g., $E^+_{p,x,t}$) according to

(A7) $\quad E^+_{a,x,t} = \sum_{\text{all } y} \Psi^E_{x,y,t} E^-_{p,y,t}$

(A8) $\quad J^+_{q,x,t} = \sum_{\text{all } y} \Psi^{Jq}_{x,y,t} P^-_{q,y,t}$

(A9) $\quad S^+_{i,q,x,t} = \sum_{\text{all } y} \Psi^S_{x,y,t} S^-_{i,q,y,t}$

(A10) $\quad A^+_{m,q,x,t} = \sum_{\text{all } y} \Psi^S_{x,y,t} A^-_{m,q,y,t}$

In this prescription, $\Psi^E_{x,y,t}$ ($\Psi^S_{x,y,t}$) represents the proportion of eggs (or settled individuals) in cell y at $t - \Delta t$ that are transported to cell x by time t. In a similar way, $\Psi^{Jq}_{x,y,t}$ represents the proportion of unsettled individuals with development index q in cell y at $t - \Delta t$ that are transported to cell x by time t.

We determine each of these quantities by tracking N_E particles per cell over $U_i - \Delta t \to U_i$. For eggs and pelagic individuals, we assume that the deterministic part of the velocity is given by the SNAC characterization (Logemann et al. 2004) of the HAMSOM model (Harms et al. 2000) and that the random components correspond to a diffusion process with coefficient Φ_P. Eggs are assumed to be located at a constant 6.3 m below the surface. Unsettled individuals who are below the settlement threshold length are assumed to be at a constant 25 m below the surface (or 70% of the local depth, whichever is less). Individuals longer than the settlement threshold but as yet unsettled are assumed to reside at 70% of the local depth. Settled individuals are assumed to be located a nominal 1 m above the bottom, and their velocity is determined by the applicable adult movement model as discussed in the main text.

Biological continuity

Eggs

We update the state of the egg population of cell x at a set of times $\{u^E_x\}$ related to each other by the requirement that

(A11) $\quad \Delta p = \int_{u^E_{x,i-1}}^{u^E_{x,i}} g^E_x(\tau) \, d\tau$

where $g^E_x(\tau)$ is the egg development rate in cell x at time τ.

The update process requires us to determine the survival of each development class since the last update ($\xi^E_{p,x,t}$). We then add all the surviving individuals from the $p = 1$ class into the first unsettled juvenile class, thus

(A12) $\quad I^+_{q_h,x,t} = I_{q_h,x,t} + \xi^E_{1,x,t} E^-_{1,x,t}$

and then move the survivors from all other classes one to the right, thus

(A13) $\quad E^+_{p+\Delta p,x,t} = \begin{cases} 0 & \text{if } p \leq \Delta p \\ \xi^E_{p,x,t} E^-_{p,x,t} & \text{if } \Delta p < p < 1 \end{cases}$

Unsettled individuals

We update the state of the unsettled juvenile population of cell x at a set of times $\{u^I_x\}$ related to each other by the requirement that

(A14) $\quad \Delta q = \int_{u^I_{x,i-1}}^{u^I_{x,i}} g^I_x(\tau) \, d\tau$

where $g^I_x(\tau)$ is the juvenile development rate in cell x at time τ.

The update process requires us to determine the survival of each development class since the last update ($\xi^I_{q,x,t}$) and the proportion of those survivors who have settled ($\rho^I_{q,x,t}$). We then move the survivors of each class who have not settled by one to the right and add the survivors who have settled to the appropriate settled class, thus

(A15) $\quad I^+_{q+\Delta q,x,t} = \begin{cases} 0 & \text{if } q \leq \Delta q_h \\ \xi^I_{q,x,t}(1 - \rho^I_{q,x,t}) I^-_{q,x,t} & \text{if } q \geq q_h \end{cases}$

(A16) $\quad S^+_{i,q+\Delta q,x,t} = S^-_{i,q+\Delta q,x,t} + \xi^I_{q,x,t} \rho^I_{q,x,t} I^-_{q,x,t}$

Settled individuals

We update the state of the settled population, whether mature or immature, of cell x at a set of times $\{u^S_x\}$ related to each other by the requirement that

(A17) $\quad \Delta q = \int_{u^S_{x,i-1}}^{u^S_{x,i}} g^S_x(\tau) \, d\tau$

where $g^S_x(\tau)$ is the settled development rate in cell x at time τ.

The update process requires us to determine the survival of each development class since the last update ($\xi^S_{q,x,t}$) and move the survivors of each class one to the right, thus

(A18) $\quad S^+_{q+\Delta q,x,t} = \begin{cases} 0 & \text{if } q < q_h \\ \xi^S_{q,x,t} S^-_{q,x,t} & \text{if } q \geq q_h \end{cases}$

Cod are moved from the immature to the mature class of settled fish at the end of each year according to the expected proportion mature at length.

We also calculate the total number of eggs produced by the settled population since the last update and add them to the first egg class, so that

(A19) $\quad E^+_{\Delta p,x,t} = E^-_{\Delta p,x,t} + \sum_{q=q_h}^{\infty} B_{q,x,t} S^-_{m,q,x,t}$

where $B_{q,x,t}$ is the number of eggs produced by an individual with development index q in cell x since the update prior to t.

Biological processes

Length and age

We compiled a data set of length against age by ICES stat squares from data supplied by Fisheries Research Services

(Marine Laboratory, Aberdeen, AB11 9DB, Scotland, unpublished data), the Centre for Ecology, Fisheries and Aquaculture Science (Pakefield Road, Lowestoft, NR330HT, England, unpublished data), and the Department of Agriculture and Regional Development (Dundonald House, Belfast BT4 3SB, Northern Ireland, unpublished data). Our model assumes that an individual confined to a specific cell would follow a von Bertalanffy growth law. To make intercell transport self-consistent, we need the asymptotic length (L_∞) to be the same for all cells. Hence we fitted the data for each cell with a length at age key

$$(A20) \quad L_x^K(a) = L_\infty - (L_\infty - L_H) \exp(-\gamma_x a)$$

thus determining a global hatch and asymptotic lengths (L_H and L_∞) and a cell-specific von Bertalanffy growth rate γ_x.

Since eq. (A20) is a continuous function, it can be used to infer a cell-dependent age at length function

$$(A21) \quad a_x^K(L) = \frac{1}{\gamma_x} \ln\left(\frac{L_\infty - L_H}{L_\infty - L}\right)$$

In a similar way, we determined global length–age and age–length keys ($L_G(a)$ and $a_G(L)$, respectively) by fitting a von Bertalanffy curve to the pooled data set; we also determined respective North Sea global keys ($L_N(a)$ and $a_N(L)$) by fitting the pooled North Sea data.

Length, weight, and development index

From the definition of development index (eq. A2), the length of an individual of development index q is

$$(A22) \quad L(q) = L_\infty - (L_\infty - L_H) \exp(-q)$$

We assume that the weight (in grams) of an individual is proportional to the cube of its length (in centimetres), so the weight of an individual with length L and development index q is

$$(A23) \quad W(L) = W_0 L^3 \quad \Leftrightarrow \quad W_q = W(L(q))$$

Egg development

Guided by the work of Page and Frank (1989) on haddock and remembering the close similarity between the eggs of cod and haddock (Daan 1978; Fox et al. 2000), we assume that cod egg development is described by

$$(A24) \quad g_x^E(t) = D_E(T_x(t) + T_E)^{P_E}$$

with the parameter values given in Table 1.

Fish development

The von Bertalanffy growth rate for each cell (γ_x) is determined from the age–length key for that cell. From the development index definition (eq. A2), we see that the appropriate development rate is the von Bertalanffy growth coefficient for the cell concerned:

$$(A25) \quad g_{x,t}^I = g_{x,t}^S = \frac{dq}{dt} = \frac{1}{L_\infty - L} \cdot \frac{dL}{dt} = \gamma_x$$

Settlement

Unsettled fish whose length exceeds a critical value L_S, that is whose development index exceeds

$$(A26) \quad q_s = \ln\left(\frac{L_\infty - L_H}{L_\infty - L_S}\right)$$

settle immediately provided only that the cell in which they reside contains a finite "settleable" area ($U_x > 0$). Hence we write

$$(A27) \quad \rho(q, x) = \begin{cases} 0 & \text{if } U_x = 0 \text{ or } q < q_s \\ 1 & \text{otherwise} \end{cases}$$

Fecundity

We use $\beta_{q,t}$ to denote the per capita fecundity rate of a mature, settled individual in development class q. Thus, if two successive settled population updates for cell x happen at times u_i and u_{i+1}, then the total per capita egg production in the interupdate interval is

$$(A28) \quad B_{q,x,u_i} = \beta_{q,u_i} A_{q,x,u_i}(u_{i+1} - u_i)$$

We assume that adults have a 1:1 sex ratio and the proportion of adults with development index q who are sexually mature is m_q. At the end of each year, before the start of the next year's spawning season, fish are moved from the immature, settled class of index q to the mature, settled class of index q, such that

$$(A29) \quad m_q = \frac{S_{m,q,x,t}}{S_{i,q,x,t} + S_{m,q,x,t}}$$

We further assume that spawning takes place only between February and April. Hence we write

$$(A30) \quad \beta_{q,t} = \begin{cases} 0.5 f_q & \text{if } t_s \leq t_y \leq t_e \\ 0 & \text{otherwise} \end{cases}$$

where t_y represents the time of year and f_q is the per capita fecundity of a female with development index q.

The size-dependent per capita fecundity rate of mature fish during the spawning season (β_q^S) was determined from the work of Marteinsdottir and Begg (2002) as

$$(A31) \quad f_q = f_0(W_q)^{P_e}$$

To determine the proportion mature at development index q, we first fit a Weibull distribution to the ICES estimates for proportion mature at age for the whole North Sea. We then transformed this into proportion mature at length using the global North Sea age–length key, thus

$$(A32) \quad m(L) = 1 - \exp\left[-\left(\frac{a_N(L)}{a_m}\right)^{P_m}\right]$$

Finally we note that we can transform length into development index using eq. (A22), thus

$$(A33) \quad m_q = m(L(q))$$

Survival

Using $u_i \equiv u_{x,i}^K$ as shorthand update times, $K \in [E, I, S]$ to denote the target population, and q as shorthand for q or p as appropriate, we write

(A34) $\zeta_{q,x,u_i}^K = \exp[-\delta_{q,x,u_i}^K(u_{i+1} - u_i)]$

Egg mortality

We assume that eggs suffer time- and position-independent mortality δ_E, whose value we calculated from the work of Rijnsdorp and Jaworski (1990), assuming that a cod egg has diameter 1.4 mm.

Unsettled fish mortality

We assume that the pelagic mortality $(\delta_{q,x,t}^P)$ is linearly related to time (t), and local yearly average temperature $(\bar{T}_{x,t})$. We assume that the coefficients in this relation are dependent on region and write

(A35) $\delta_{x,t}^P = \delta_0^{PR} + \delta_T^{PR}\bar{T}_{x,t} + \delta_Y^{PR}Y$

where

(A36) $Y = \mathrm{trunc}(t/365)$

Mortality for fish which are large enough to settle $(L > L_S;$ i.e., $q > q_s)$ but who have not done so because they are in a cell with no settleable area are subject to excess mortality based on the natural mortality for settled individuals of the same size. Hence we write

(A37) $\delta_q^I = \begin{cases} \delta_{x,t}^P & \text{if } q < q_s \\ \delta_N^S(q)\exp\left[\dfrac{L(q) - L_S}{L_{cm}}\right] & \text{otherwise} \end{cases}$

Settled fish mortality

We assume that the per capita per-unit-time mortality rate of settled fish has three components — natural mortality (δ_N^S), fishing mortality (δ_F^S), and density-dependent mortality (δ_K^S) — so that

(A38) $\delta^S = \delta_N^S + \delta_F^S + \delta_K^S$

We obtain δ_N^S as a function of age by fitting a power function through the ICES estimates of background mortality at age for the North Sea. We then transform this into mortality at length using the global North Sea age–length key and finally into a mortality at development index, using eq. (A2). The final result is

(A39) $\delta_N^S(q) = \delta_{N0}^S(a_N(L(q)))^{P_n}$

We describe δ_F^S as the product of a development-index selectivity factor C_q, a region- and year-dependent overall fishing mortality F_t^R, and a time-independent fishing effort distribution factor E_x, thus

(A40) $\delta_F^S = C_q F_t^R$

To calculate the yearly mortality and size selectivity, we used the method outlined by Cook (1998). We obtained a first estimate of F_t^R by averaging ICES yearly estimates of fishing mortality over ages 1 to 6. We then determined the age selectivity inherent in each mortality at age estimate by

dividing it by F_t^R and averaged these over all regions for the period 1990–1999 to obtain our final estimate of age selectivity. Finally, this was transformed into a continuous q selectivity function using the global age–length key and interpolating linearly between points. We then recalculated the F_t^R values using the ICES mortality at age estimates for the region and year concerned and our estimated age-selectivity.

To define the δ_K^S component, we first define the total settled biomass in cell x as

(A41) $W_{x,t}^S = \sum_{\text{all } q} S_{q,x,t} W(q)$

If U_x denotes the settleable area in cell x and $K_{x,t}$ denotes its specific carrying capacity at time t, then we design the density-dependent mortality to act only when $W_{x,t}^S$ exceeds $U_x K_{x,t}$ and then to return the local settled biomass to the local carrying capacity as rapidly as possible. Thus we write

(A42) $\delta_K^S(q) = \delta_N^S(q)\left(\dfrac{W_{x,t}^S}{U_x K_{x,t}} - 1\right)^+$

where $x^+ \equiv \max(x,0)$.

We assume that the cell-specific carrying capacity $(K_{x,t})$ is linearly related to t and $\bar{T}_{x,t}$. We assume that the coefficients in this relation are dependent on region and write

(A43) $K_{x,t} = K_0^R + K_T^R \bar{T}_{x,t} + K_Y^R Y$

where

(A44) $Y = \mathrm{trunc}(t/365)$

The parameter values determined from literature sources are shown (Appendix A Table A1).

Appendix A references

Andrews, J., Blythe, S., and Gurney, W. 2004. Stability analysis of a continuous age structured model with specific reference to North Sea cod. J. Biol. Syst. **12**: 249–260.

Cook, R.M. 1998. A sustainability criterion for the exploitation of North Sea cod. ICES J. Mar. Sci. **55**: 1061–1070.

Daan, N. 1978. Changes in cod stocks and cod fisheries in the North Sea. Rapp. P.-V. Reun. Cons. Int. Explor. Mer, **172**: 39–58.

Fox, C., O'Brien, C., Dickey-Collas, M., and Nash, R. 2000. Patterns in the spawning of cod (*Gadus morhua* L.), sole (*Solea solea* L.), plaice (*Pleuronectes platessa* L.,) in the Irish Sea as determined by generalised additive models. Fish. Oceanogr. **9**: 33–49.

Harms, I., Heath, M., Bryant, A., Backhaus, J., and Hainbucher, D. 2000. Modelling the Northeast Atlantic circulation: implications for the spring invasion of shelf regions by *Calanus finmarchicus*. ICES J. Mar. Sci. **57**: 1694–1707.

Logemann, K., Backhaus, J., and Harms, I. 2004. SNAC: a statistical emulator of the north-east Atlantic circulation. Ocean Modell. **7**: 97–110.

Marteinsdottir, G., and Begg, G. 2002. Essential relationships incorporating the influence of age, size and condition on variables required for estimation of reproductive potential in Atlantic cod *Gadus morhua* stocks. Mar. Ecol. Prog. Ser. **235**: 235–256.

Page, F., and Frank, K. 1989. Spawning time and eggs stage duration in Northwest Atlantic haddock (*Melanogrammus aeglefinus*)

Table A1. Parameter values and sources.

Symbol	Name	Value	Unit	Source
Weight, length, and development				
W_0	Weight/length scale	0.104	$gm \cdot cm^{-1}$	—
L_∞	Asymptotic length	197	cm	—
L_H	Length at hatch	0.14	cm	—
L_S	Settlement length	3.5	cm	—
Eggs				
D_E	Deviance scale	0.129	$day^{-1}(^\circ C)^{-P_E}$	Page and Frank 1989
P_E	Deviance power	0.89	—	Page and Frank 1989
T_E	Deviance offset	2.0	$^\circ C$	Page and Frank 1989
δ_E	Egg mortality	0.232	day^{-1}	Rijnsdorp and Jaworski 1990
Settled fish				
δ_{N0}^S	Background mortality scale	0.003	$day^{-1} \cdot year^{-P_n}$	—
p_n	Background mortality power	—	—	—
L_{cm}	Excess mortality length	2	cm	—
Spawning				
t_s	Spawning start	32	day (of year)	—
t_e	Spawning end	121	day (of year)	—
f_0	Fecundity scale	73.09	$eggs \cdot female^{-1}$	Marteinsdottir and Begg 2002
p_e	Fecundity power	1.248	—	Marteinsdottir and Begg 2002
p_m	Maturity power	3.984	—	Andrews et al. 2004
a_m	Maturity age scale	4.118	years	Andrews et al. 2004

stocks with emphasis on Georges and Browns bank. Can. J. Fish. Aquat. Sci. **46**(Suppl. 1): 68–81.

Rijnsdorp, A., and Jaworski, A. 1990. Size-selective mortality in plaice and cod eggs — a new method in the study of egg mortality. J. Conseil, **47**: 256–263.

Speirs, D., Gurney, W., Heath, M., and Wood, S. 2005. Modelling the basin-scale demography of *Calanus finmarchicus* in the North-east Atlantic. Fish. Oceanogr. **14**: 333–358.

Appendix B. Estimating the spatial spawning stock biomass distribution.

In the first quarter of year y, a series of $v_{x,y}$ surveys is conducted in stat square x, which lies within region R. In survey i ($\in (1, v_{x,y})$), gear of type G, which sweeps a distance $M_G/2$ either side of its centre line, is towed for a distance T_G metres, thus sweeping out a total area $A_G = M_G T_G$ m^2. The sample contains $N_{s,y}^{i,L}$ individuals in length class L. If we assume that a proportion κ_G^L of individuals in this length class who encounter the trawl are retained, then we can infer that the average density of such individuals across stat square x in year y is

$$(B1) \quad \rho_{x,y}^L = \frac{1}{v_{x,y}} \sum_{i=1}^{v_{x,y}} \frac{N_{x,y}^{i,L}}{A_G \kappa_G^L}$$

Our attempts to determine the gear-specific catchability coefficients, κ_G^L, from first principles were unsuccessful, so to proceed further we noted that if the settleable area of cell x is U_x, then the total abundance of age class a fish in region R in year y is

$$(B2) \quad P_{R,y}^a = \sum_{x \in R} \sum_{L_x^K(a)}^{L_x^K(a+1)} \rho_{x,y}^L U_x$$

In principle, the ICES estimates of regional age class abundance are exactly comparable with the estimates inferred using eq. (B2), so we used numerical optimization to determine the catchabilities that made the survey abundances match as closely as possible to the yearly series of ICES assessments for the period 1990–1999. We show the resulting best-fit catchabilities for the grande overture verticale trawl, 4 m beam trawl, rockhopper trawl, and Portuguese high headline trawl (Appendix B Table B1).

Once we have determined the catchabilities, we can estimate the spawning stock biomass in cell x in the first quarter of year y using our estimates of weight and proportion mature at length (eqs. A23 and A32). However, when the estimates thus obtained are summed to obtain a regional spawning stock biomass ($B_{R,y}^S$), the results are seldom consistent with the ICES working group's estimate of regional spawning stock biomass ($B_{R,y}^I$). Further, there is not enough data or sufficient control in the fitting of the model to be sure of yearly spatial variations, thus we estimate an average spatial distribution over the 8 years. Thus we define

$$(B3) \quad \rho_{x,\bar{y}}^L = \frac{1}{\sum_{y=1991}^{1998} v_{x,y}} \sum_{y=1991}^{1998} \sum_{i=1}^{v_{x,y}} \frac{N_{x,y}^{i,L}}{A_G \kappa_G^L}$$

Table B1. Fitted catchabilities for various gear types.

Fish length (cm)	GOV$_{\text{not Scotland}}$	GOV$_{\text{Scotland}}$	4mB	RHT	PHHT
<20	0.306	0.012	1.000	0.181	0.180
20–29	0.395	0.016	1.000	0.833	0.039
30–39	0.480	0.132	0.998	0.994	0.224
40–49	0.277	0.074	0.997	0.304	0.047
50–59	0.366	0.182	0.975	0.488	0.631
60–69	0.479	0.338	0.993	0.067	0.086
70–79	0.495	0.391	1.000	0.199	0.324
80–89	0.989	0.915	0.825	0.153	0.151
90–99	0.995	0.955	0.995	0.074	0.141
>100	1.000	0.981	0.999	0.000	0.104

Note: GOV, grande overture verticale trawl; 4mB, 4 m beam trawl; RHT, rockhopper trawl; PHHT, Portuguese high headline trawl.

Hence we write our best estimate of spawning stock biomass in cell x in year y as

$$\text{(B4)} \quad B_{x,y}^S = \frac{1}{\theta_y^R} \sum_{\text{all } L} \sum_{\text{all } y} \rho_{x,\bar{y}}^L \, U_x W(L) m(L)$$

where

$$\text{(B5)} \quad \theta_y^R = \frac{1}{B_{R,y}^I} \sum_{x \in R} \sum_{\text{all } L} \rho_{x,y}^L W(L) m(L)$$